



# SAPHYRE

Contract No. FP7-ICT-248001

## System Level Evaluation Methodology and Asymptotic Analysis Assessment D4.3

|                   |  |
|-------------------|--|
| Contractual date: | M24  |
| Actual date:      | M24  |
| Authors:          | Haibin Zhang, Jianhui Li, Lars Thiele, Leonardo Badia, Ljupčo Jorguŝeski, Luca Anchora, Martin Schubert, Michał Szydełko |
| Participants:     | CFR, FhG, TNO, TUIL, WRC   |
| Work package:     | WP4  |
| Security:         | Public   |
| Nature:           | Report   |
| Version:          | 1.1  |
| Number of pages:  | 50   |

### Abstract

This deliverable provides an overview on the simulation methodologies developed in WP4 of the SAPHYRE project. The overall project goal is to achieve demonstrate gains from sharing resources and infrastructure. The sharing gain depends on different system functionalities, thus a cross-layer approach is required that involves different aspects like physical layer optimization, medium access control, and system level simulations. The results provide the basis for joint system level simulation in the 3rd year of SAPHYRE.

### Keywords

Resource allocation, scheduling, system level simulation, asymptotic analysis.



# Contents

|          |   |           |
|----------|---|-----------|
| <b>1</b> | <b>Executive Summary</b>  | <b>3</b>  |
| <b>2</b> | <b>Joint PHY–MAC Modelling and Performance Measures</b>                 | <b>5</b>  |
| 2.1      | Scheduling and Beamforming . . . . .                                    | 5         |
| 2.1.1    | Downlink System Model . . . . .   | 5         |
| 2.1.2    | Decentralized Scheduling for Limited Feedback Systems . . .             | 7         |
| 2.1.3    | Scenario Definition . . . . .   | 10        |
| 2.1.4    | Co-located Base Stations (BSs) . . . . .                                | 10        |
| 2.1.5    | Distributed BSs . . . . .   | 10        |
| 2.1.6    | Simulation Model . . . . .  | 10        |
| 2.1.7    | Initial Results and Discussion . . . . .                                | 11        |
| 2.2      | Relaying and Beamforming . . . . .                                      | 15        |
| 2.3      | Network Layout, Propagation Environment, and Traffic Characteristics 18 |           |
| 2.3.1    | Network layout . . . . .  | 18        |
| 2.3.2    | Performance Metrics Definition . . . . .                                | 22        |
| <b>3</b> | <b>System Level Evaluation</b>  | <b>25</b> |
| 3.1      | Multi-Operator Multi-Cell Simulation Based on NS3 . . . . .             | 25        |
| 3.1.1    | Tool description . . . . .  | 25        |
| 3.1.2    | System model . . . . .  | 26        |
| 3.1.3    | Simulation scenario . . . . .   | 30        |
| 3.1.4    | Example Simulation Results . . . . .                                    | 32        |
| 3.2      | Simulation Framework for Evaluating Game-Theoretic Strategies . .       | 37        |
| 3.2.1    | Network layout . . . . .  | 37        |
| 3.2.2    | Scheduler design . . . . .  | 40        |
| 3.3      | Asymptotic Analysis Assessment . . . . .                                | 42        |
| <b>4</b> | <b>Conclusions and Discussion of Next Steps</b>                         | <b>47</b> |
|          | <b>Bibliography</b>   | <b>49</b> |



## Abbreviations

|                 |   |
|-----------------|---|
| <b>16 QAM</b>   | 16 Quadrature Amplitude Modulation (QAM)      |
| <b>64 QAM</b>   | 64 QAM  |
| <b>BS</b>       | Base Station                                  |
| <b>CQI</b>      | Channel Quality Indicator                     |
| <b>CSI</b>      | Channel State Information                     |
| <b>CSIT</b>     | Channel State Information at the Transmitter  |
| <b>DFT</b>      | Discrete Fourier Transform                    |
| <b>EESM</b>     | Exponential Effective SINR Mapping            |
| <b>eNB</b>      | Evolved Node B                                |
| <b>IIR</b>      | Infinite Impulse Response                     |
| <b>IRC</b>      | Interference Rejection Combining              |
| <b>ISD</b>      | inter-Site Distance                           |
| <b>LTE</b>      | Long Term Evolution                           |
| <b>MAC</b>      | Medium Access Control                         |
| <b>MCS</b>      | Modulation and Coding Scheme                  |
| <b>MMSE</b>     | Minimum Mean Square Error                     |
| <b>MNO</b>      | Mobile Network Operator                       |
| <b>MRC</b>      | Maximum Ratio Combining                       |
| <b>MU-MIMO</b>  | Multi-User MIMO                               |
| <b>NS3</b>      | Network Simulator 3                           |
| <b>OC</b>       | Optimum Combining                             |
| <b>OFDM</b>     | Orthogonal Frequency Division Multiplex       |
| <b>OFDMA</b>    | Orthogonal Frequency Division Multiple Access |
| <b>PHY</b>      | Physical Layer                                |
| <b>PMI</b>      | Precoding Matrix Indicator                    |
| <b>PRB</b>      | Physical Resource Block                       |
| <b>PSS</b>      | Primary Synchronization Signal                |
| <b>QAM</b>      | Quadrature Amplitude Modulation               |
| <b>QPSK</b>     | Quadrature Phase Shift Keying                 |
| <b>QoS</b>      | Quality of Service                            |
| <b>QuaDRiGa</b> | Quasi Deterministic Radio Channel Generator   |
| <b>RAT</b>      | Radio Access Technology                       |
| <b>RB</b>       | Resource Block                                |
| <b>RET</b>      | Remote Electrical Tilt                        |

## *Abbreviations*

|             |  |
|-------------|--|
| <b>RS</b>   | Relay Station                          |
| <b>RSRP</b> | Reference Signal Received Power        |
| <b>RSSI</b> | Received Signal Strength Indicator     |
| <b>SCME</b> | Spatial Channel Model Extended         |
| <b>SINR</b> | Signal-to-Interference-and-Noise Ratio |
| <b>TTI</b>  | Transmission Time Interval             |
| <b>UE</b>   | User Equipment                         |
| <b>UT</b>   | User Terminal                          |
| <b>VoIP</b> | Voice over IP                          |
| <b>ZF</b>   | Zero-Forcing                           |

# 1 Executive Summary

This deliverable provides an overview on the simulation methodologies developed in Task 4.3 of the SAPHYRE project [9]. The overall goal is to evaluate the system level performance, and especially the gains that are obtained from the *sharing strategies* developed in SAPHYRE.

Sharing enables a more efficient exploitation of the available system resources. This comes at the cost of increasing the system complexity. If operators want to share a resource, then they must take measures against mutual interference. Therefore, the task of sharing cannot be solely viewed from a system-layer perspective. It also crucially depends on the Physical Layer (PHY) and the Medium Access Control (MAC), where interference can be reduced and/or avoided by signal processing techniques (e.g. MIMO, beamforming) and resource allocation.

Therefore, the simulation methodologies in SAPHYRE need to take in account the *cross-layer* nature of the sharing strategies. In order to assess the system level performance, the following fundamental system functionalities need to be considered:

- Modelling of the multi-antenna vector channel and the resulting interference (network topology, propagation, traffic, etc.). This is partly based on the interference models derived in WP2.3 (see Deliverable D2.3).
- Interference avoidance techniques from WP2.
- Signal processing techniques from WP3 (beamforming, MIMO, relaying).
- Cross-Layer optimisation techniques from WP4.

The lower layer modelling is mostly carried out with Matlab [?]. The methodologies are described in Chapter 2. This provides the basis for the system level simulations, which are mostly carried out with Network Simulator [8]. In addition, asymptotic analysis and semi-analytical assessment will address simplified network deployment and a reduced set of involved parameters, aiming to provide insight on the impact of critical parameters and reveal fundamental trends and limitations.

The key contributions of this report are summarised as follows.

- A decentralised scheduling framework is developed in Section 2.1. Different scheduling strategies are developed, which include a certain degree of user fairness. Also, different sharing scenarios are modelled, e.g. with co-located or distributed locations of different BS as well as different degree of Channel State Information (CSI) at the transmitter side. Initial results are described in Subsection 2.1.7 along with a brief conclusion and an outlook on the next steps.

## 1 Executive Summary

- In Section 2.2, a quasi-static (or snap-shot) system level simulator is developed using MATLAB. It is used to investigate the advanced physical layer signal processing techniques such as transmit beamforming or complicated receiver concept. It is also suitable for system function such as fast adaptive resource scheduling. As an initial test, we investigate the relay assisted resource sharing between two operators in the Manhattan grid, where the transmission between the base station and the users are assisted by four relays for each operator.
- In Section 3.2, a framework for simulating the HSPA radio access technology is presented. The goal of this simulation is to prove game theoretic based SAPHYRE concepts of the spectrum sharing, by quantitative evaluation of system level performance measures with respect to the reference cases. Based on the simulation results generated in the simulation environment, we will demonstrate the SAPHYRE gains coming from the short term spectrum auctioning in the HSPA network, where resource sharing between the Mobile Network Operator (MNO)'s provides a gain in terms of improved spectrum utilisation and increased throughput on the system level.
- In Section 2.3, the modelling of network Layout, propagation environment, and traffic characteristics is discussed. More specifically, the following results are included:
  - System-level modelling: approaches of modelling network layout (for both homogeneous and heterogeneous deployments), propagation modelling taking into account large-scale fading (e.g. distance-based path loss, shadowing, etc.), and traffic modelling (either uniformly or non-uniformly distributed).
  - Performance metrics, including gains (of sharing), system overhead, fairness among users of different operators, and complexity introduced by sharing.

The system-level simulator was built with the Delphi programming language.

- Section 3.1 describes the system level simulations, based on the open source network simulator (Network Simulator 3 (NS3)). To this end, NS3 was customised. The support to multi-operator multi-cell scenarios has been introduced, together with the software architecture necessary for evaluating spectrum sharing policies.
- Section 3.3 presents an asymptotic analysis on the orthogonal spectrum sharing case. The results are obtained by implementing and evaluating (through the aforementioned simulator) an upper-bound algorithm.

## 2 Joint PHY–MAC Modelling and Performance Measures

The evaluation of the system level performance hinges on the PHY and MAC layer, which are strongly affected by sharing of resources and infrastructure. By using signal processing methods for interference avoidance/reduction, and by properly allocating the resources, it is possible to achieve co-existence of multiple operators on the same resource. This is known as non-orthogonal sharing. But also the performance of orthogonal sharing depends crucially on the way PHY and MAC are modeled. Hence, part of the SAPHYRE activities focus on the joint modelling and optimisation of PHY and MAC

### 2.1 Scheduling and Beamforming

In the first phase of this project we investigated the simplest way of spectrum sharing which is realized by decentralized scheduling where User Equipment (UE)s provide Long Term Evolution (LTE) compliant feedback such as Channel Quality Indicator (CQI) and Precoding Matrix Indicator (PMI). Therefore, we introduce in Subsection 2.1.1 a system model for Orthogonal Frequency Division Multiple Access (OFDMA) based and spatial precoded cellular downlink transmission. At this stage our main focus is on different scheduling strategies including certain degree of user fairness described in Subsection 2.1.2. Furthermore, we treat different sharing scenarios, e.g. with co-located or distributed locations of different BS as well as different degree of CSI at the transmitter side. The scenario description is given in Subsection 2.1.3 whereas at the current state of the project only the first one is considered. The underlying simulation model and assumptions as well as the main characteristics of the Quasi Deterministic Radio Channel Generator (QuaDRiGa). Finally initial results are described in Subsection 2.1.7 along with a brief conclusion and an outlook on the next steps.

#### 2.1.1 Downlink System Model

In following paragraph, we use a multi-antenna OFDMA downlink model for cell-independent, linear precoded transmission using predefined *codebook* entries according to LTE specifications. This implies that each BS may transmit up to  $N_t$  *data streams* simultaneously on the same resource, while each UE may receive up to  $N_r$  streams simultaneously. Clearly, there is the degree of freedom that a BS may serve many UEs with fewer streams each, or fewer UEs with more streams each, which we will explore later. As we are observing *non-cooperative* downlink transmission, this means that each stream may only be transmitted from a single BS.

In the sequel, let us observe UE  $k$  which is served by BS  $m$ . While the set  $\mathcal{K}$  captures  $K$  UEs, we denote  $\mathcal{K}_m \subset \mathcal{K}$  as the set of all UEs served by BS  $m$  per time

instance. Note, the number of UEs which are simultaneously served on the same frequency resource is obviously limited to the number of BS transmit antennas, e.g.  $|\mathcal{K}_m| \leq N_t$ . Therefore, let us assume a scheduling algorithm which selects a subset of active users per Resource Block (RB) according to a specific metric. Thus, the received downlink signal  $\mathbf{y}_{k,t}$  for  $t \in \mathcal{T}_{s,k} \subset \mathcal{T}_s$  at user  $k$  in the cellular environment is given by

$$\begin{aligned} \mathbf{y}_{k,t} = & \underbrace{\mathbf{H}_{m,k} [\mathbf{B}_{m,k}]_{:,t} \sqrt{p_{m,t}} x_{m,t}}_{\bar{\mathbf{h}}_{k,t}} + \underbrace{\sum_{j \in \mathcal{T}_s \setminus \{t\}} \mathbf{H}_{m,k} [\mathbf{B}_m]_{:,j} \sqrt{p_{m,j}} x_{m,j}}_{\substack{\text{Intra-cell interference} \\ \boldsymbol{\vartheta}_{k,t}}} \\ & + \underbrace{\sum_{l \in \mathcal{M} \setminus \{m\}} \sum_{j=1}^{N_t} \mathbf{H}_{l,k} [\mathbf{B}_l]_{:,j} \sqrt{p_{l,j}} x_{l,j}}_{\substack{\text{Inter-cell interference} \\ \mathbf{z}_k}} + \mathbf{n} \end{aligned} \quad (2.1)$$

where  $\mathbf{H}_{m,k}$  is the channel between UE  $k$  and the  $m$ -th BSs,  $\mathbf{B}_{m,k}$  is the compound precoding vector used to serve UE  $k$ , and  $[\mathbf{B}_{m,k}]_{:,t}$  is the sub-portion, i.e. the  $t$ -th data stream, of the precoders intended for user  $k$ . We write as  $\bar{\mathbf{H}}_k$  the *effective* channel between UE  $k$  and its serving BS after precoding, which consists of multiple, i.e.  $|\mathcal{T}_{s,k}|$  column vectors  $\bar{\mathbf{h}}_{k,t}$  such that  $\bar{\mathbf{H}}_k = [\bar{\mathbf{H}}_{k,1} \dots \bar{\mathbf{H}}_{k,|\mathcal{T}_{s,k}|}]$ . The corresponding potential data streams stacked in  $\mathbf{x}_k = [x_{m,t} \dots x_{m,|\mathcal{T}_{s,k}|}]$  and  $\mathbf{x} \sim \mathcal{N}_{\mathbb{C}}(\mathbf{0}, \mathbf{I})$  are distorted by the intra-cell and inter-cell interference aggregated in  $\boldsymbol{\vartheta}_{k,t}$  and  $\mathbf{z}_k$ , respectively. Each BS  $m$  may select a limited number  $|\mathcal{T}_s| \leq N_t$  of active beams to serve one user with multiple beams or multiple users simultaneously.

In case of LTE transmission concepts, this is done by choosing the corresponding precoding columns from a pre-defined beam alphabet  $\mathbf{B}_\omega$ . In the case of  $N_t = 2$ , beam alphabet size  $\Omega = 2$  and Discrete Fourier Transform (DFT)-based precoding, this can be either

$$\mathbf{B}_1 = \frac{1}{\sqrt{2}} \begin{bmatrix} 1 & 1 \\ i & -i \end{bmatrix} \quad \text{or} \quad \mathbf{B}_2 = \frac{1}{\sqrt{2}} \begin{bmatrix} 1 & 1 \\ 1 & -1 \end{bmatrix}. \quad (2.2)$$

Columns in  $\mathbf{B}$  representing streams that are currently not used are simply filled with zeros. Note that  $\mathbf{B}$  has to be scaled depending on the choice of  $|\mathcal{T}_s|$  in order to fulfill a *per base station power constraint*, i.e.  $\text{tr}\{\mathbf{B}_m \mathbf{B}_m^H\} \leq p_m$ . If only one beam is active, i.e.  $|\mathcal{T}_s| = 1$ , we call it single-stream transmission mode, while for  $|\mathcal{T}_s| > 1$ , we refer to it as multi-stream transmission mode. Figure 2.1 depicts the resulting beam patterns for  $N_t = 4$  transmit antennas at the BS. The precoders are generated according to (2.2) or based on the current LTE specification [11] suggesting Householder beams. The scheduling entity will select the corresponding beams and allocate an equal fraction of transmit power to the active beams.

The resulting Signal-to-Interference-and-Noise Ratio (SINR) is determined using a suitable receive beamforming vector  $\mathbf{w}_{k,t}$ , e.g. Maximum Ratio Combining (MRC) or Optimum Combining (OC), and the following expression

$$\text{SINR}_{k,t} = \frac{\mathbf{w}_{k,t}^H \bar{\mathbf{h}}_{k,t} \bar{\mathbf{h}}_{k,t}^H \mathbf{w}_{k,t}}{\mathbf{w}_{k,t}^H \mathbf{z}_{k,t} \mathbf{w}_{k,t}}, \quad (2.3)$$

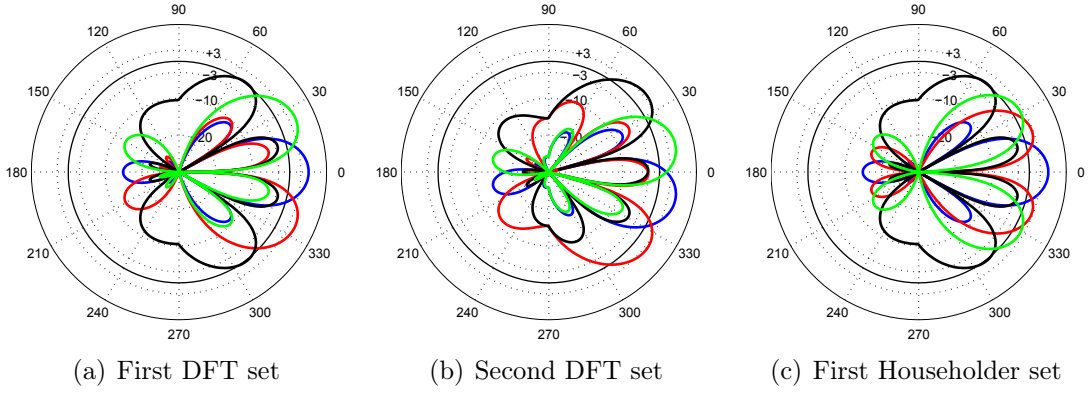


Figure 2.1: Radiation patterns for  $N_t = 4$  transmit antennas and  $\lambda/2$  antenna spacing. Figures from left to right show first and second DFT set (similar to (2.2)) and the first set of Householder beams, refer to LTE specification [11].

where  $\mathbf{Z}_{k,t}$  combines the intra- and inter-cell interference  $\mathbf{v}_{k,t}$  and  $\mathbf{z}_k$ , respectively. These SINRs are mapped into corresponding Modulation and Coding Scheme (MCS) using the Exponential Effective SINR Mapping (EESM) and common LTE mapping curves for Quadrature Phase Shift Keying (QPSK), 16 QAM (16 QAM) and 64 QAM (64 QAM) with different code rates.

### 2.1.2 Decentralized Scheduling for Limited Feedback Systems

Let us consider a set of users  $K = |\mathcal{K}|$  UEs assigned to a BS. To decide for the used transmission mode and the particular radio resource assignment, the BS evaluates the feedback reported by the UEs. This may be done using different scheduling algorithms.

**The round-robin metric** is a simple algorithm is to serve the users by assigning time and/or frequency resources one after each other to a different user. After  $K$  resources, the same user is served again. This is a simple way to ensure fairness but it is known to be suboptimal in terms of data throughput because channel conditions are not taken into account. Since time and frequency resources of different users may show independent fading, a channel-dependent resource assignment will be beneficial.

**The maximum throughput metric** is assigning the resources to the users with highest CQIs. At this stage spatial mode adaptation can be included as well. This adds a spatial dimension to the already available resources defined in time and frequency. In case that an additional spatial layer can improve the system throughput, the BS is loading another spatial layer using a specific precoding strategy. On the other hand, maximizing the throughput cannot meet *fairness* requirements. In a multi-cell environment, there is a certain spread of the effective SINRs at the different UEs. Since fairness is a soft term, it is important that the scheduling algorithms

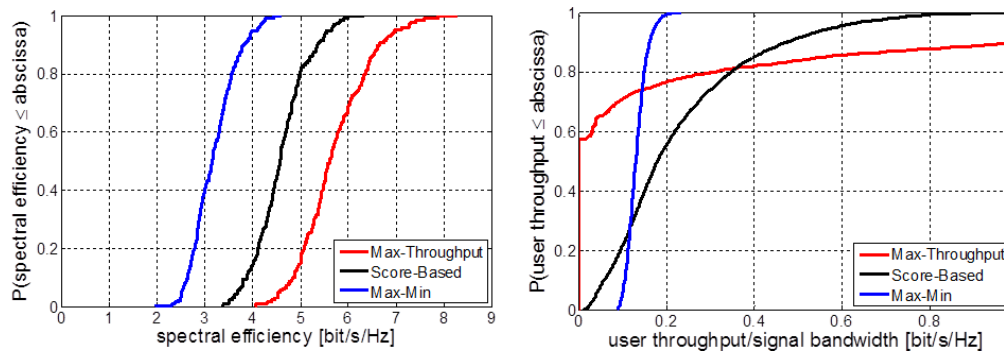


Figure 2.2: High-level overview on achievable system (left) and user data rates (right) using different scheduling strategies.

can cover different degree of fairness.

**The max-min metric** targets at maximizing the throughput of the worst users. The fairness is achieved in terms of an equivalent data rate for each user. [22] describes an algorithms which we implemented for comparison.

**The score-based metric** is a heuristic scheduling algorithm tending to assign distinct users to their best Physical Resource Blocks (PRBs) or groups of PRBs, while simultaneously ensuring instantaneous fairness in each time slot. Each user independently ranks all its PRBs by the achievable throughput, in a descending manner, based on the post-equalization SINRs for all physical layer modes. Corresponding scores chosen from a unique set are assigned. The fairness is achieved in terms of an equivalent amount of resources for all active users. Thus each user may realize an equivalent fraction of his total achievable data rate. The score-based scheduling metric asymptotically realizes a performance similar to the proportional fair scheduler [25], see [14].

### Score-Based Scheduling and Spatial Mode Adaptation

Resource allocation and selection of the proper spatial transmission modes, i.e. either single-stream transmission or multi-stream transmission, can be conveniently carried out by a score-based scheduling process developed in [14, 23], which is briefly described as follows: In a first step, the user terminals evaluate the current channel conditions per PRB in terms of their achievable SINR conditions. By using equation (2.3) in combination with the desired receive beamformer  $w_{k,t}$  and a suitable SINR-to-rate mapping function widely known as link-2-system interface, they can determine for each transmission mode the expected data rate per supported beam. This information is conveyed as CQIs to the base station, where a score-based resource scheduling algorithm is carried out.

**Spatial mode adaptation** requires a direct comparison of the per-beam rates from different spatial modes, the different data rates need to be weighted according to

the number of active spatial layers. This accounts for the higher power allocated to the single-stream transmission beam compared to multi-stream transmission mode. In particular, let  $\mathcal{T}_s$  be the set of active spatial layers for downlink service at the BS of interest. The general rationale behind the weighting factors is as follows: As we aim for a high-user throughput, spatial mode selection should favor transmission mode with  $|\mathcal{T}_s| < N_t$  whenever the user rate can be expected to be larger than the rate expected in full multi-stream transmission mode, i.e.  $|\mathcal{T}_s| = N_t$ . Consider that if a user globally decides for multi-stream transmission mode with a set of  $\mathcal{T}_s$  active beams, the available spatial streams increased by a factor  $|\mathcal{T}_s|$  with respect to the single-stream transmission mode. As a general result from that, we can assume that the user will also be assigned  $|\mathcal{T}_s|$  times the spatial resources he would get if he globally selected single-stream transmission mode. Hence, from a single-user point of view, we can conclude that decision in favor of certain spatial transmission mode at user  $k$  should be taken according to

$$\mathcal{T}_{s,k} : \arg \max_{\mathcal{T}_s \subset \mathcal{T}} \left( \arg \max_{t \in \mathcal{T}_s} (|\mathcal{T}_s| \text{rate}(\text{SINR}_{k,t})) \right) \quad (2.4)$$

The rational clearly prefers Multi-User MIMO (MU-MIMO) transmission with a single data stream per user. However, the selection scheme can be easily adapted to favor multi-stream transmission per UE by taking the sum-rate over the  $t$  strongest data streams for user  $k$  into account. Depending on the desired amount of feedback, each UE could perform a selection of CQI values for feedback provisioning using (2.4). This rational can be employed to choose between multiple codebooks with the same amount of spatial layers and/or different  $|\mathcal{T}_{s,k}|$ . Note, there is a trade-off between amount of feedback and gains from MU-MIMO, especially if feedback is reduced to a minimum.

For each user, the (weighted) per-beam rates from all modes over all PRBs are ranked by their quality, and corresponding scores are assigned. Mode selection and resource assignment is then done for each PRB individually: Firstly, each beam available per transmission mode is assigned to the user providing minimum, i.e. best score for that beam. Thereafter, the mode is selected which corresponds to the minimum overall user score.

The objective of this score-based resource allocation process is to assign each user to his best resources, and the decision on the spatial mode is taken under the premise of achieving a high throughput for each user. Clearly, the process is of heuristic nature, and hence the global scheduling target of assigning each user an equal amount of resources is achieved on average only or if the number of available resources tends to infinity. However, its convenient property for practical applications is its flexible utilization, as the set of resources can be defined over arbitrary dimensions (time/frequency/space). Thus, fairness with respect to an equal amount of resources for all active users can be established on a small time scale, e.g. even for the scheduling of resources contained within a single Orthogonal Frequency Division Multiplex (OFDM) symbol.

### 2.1.3 Scenario Definition

In this section a definition of the scenarios is given. We distinguish the scenarios by the geographic location of the BSs which can be either co-located or distributed. For the first scenario only LTE compliant limited feedback is assumed as described in Subsections 2.1.1 and 2.1.2 whereas for the distributed case a comparison for full CSI with Zero-Forcing (ZF) precoding is planned.

### 2.1.4 Co-located BSs

For the co-located BSs case two modes are considered. First no spectrum sharing is assumed as a baseline scenario in which each BS can operate only on its own 10 MHz and is henceforth referred to as **SC0**. The second mode takes full sharing of spectrum into account which means that BSs jointly select their users to be served and labeled as **SC1**. Note that there in we do not serve more users than in the non sharing case for the sake of comparability.

### 2.1.5 Distributed BSs

Distributed BSs, hexagonal deployment but shifted by a certain value as can be seen in Figure 2.9. In the same matter as before the non spectrum sharing mode is taken for baseline results. In spectrum sharing case a certain bandwidth part is used by both operators. The shared pool of spectrum is adjusted to either joint or maximum selection of UEs by each BS. In the distributed scenario a comparison of limited feedback and full CSI with ZF precoding will be provided.

### 2.1.6 Simulation Model

In the following subsection, we describe our system-level simulation tool. Since we plan to introduce measured channel coefficients from the Berlin LTE-Advanced Testbed into our simulation tool, we have to take care for an appropriate and accurate continuous generation of additional interfering BS sites, refer to figure 2.3.

These channels will be generated using a typical urban channel model, such as Spatial Channel Model Extended (SCME) [10]. However, it turned out that some mandatory features are not available yet. For that reason, we spend much effort in designing an advanced channel and scenario model for future radio systems. While the core-part is still based on the recommendation from [10], we have three main extensions included:

1. According to [15], we generate geo-correlated parameter maps for all required large-scale fading coefficients, such as delay spreads, shadow fading, k-factors and angular spreads in azimuth and elevation.
2. We include precise modeling of directional base station antennas with Remote Electrical Tilt (RET) units. Here we use a 3D-model of a Kathrein 80010541

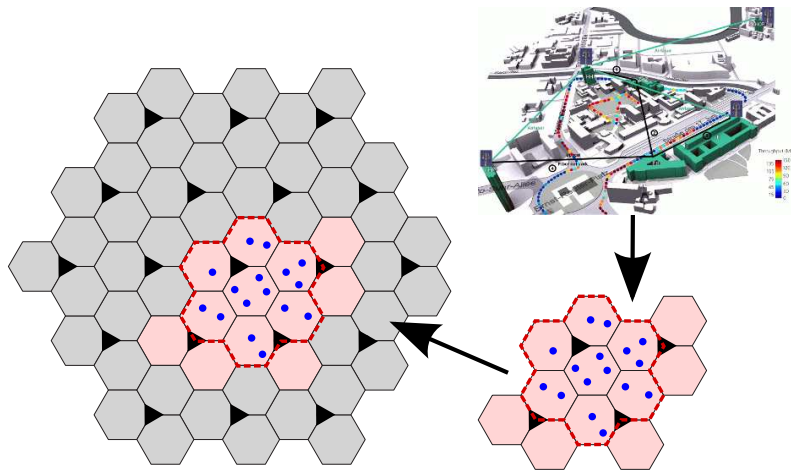


Figure 2.3: The simulation methodology of partner FhG-HHI in SAPHYRE project. Grey shaded area is obtained by emulated channel coefficients, while highlighted are can be either represented by emulated or measured channel matrices.

antenna<sup>1</sup>. More details on antenna modeling and its impact on cellular system performance evaluation can be found in [24].

3. Quasi-deterministic channel's time evolution with drifting of multi-path scattering objects. Figures 2.4(a) and 2.4(b) depict the two 2D cuts of radiation patterns, both in elevation and azimuth direction.

A detailed list of the multi-cell channel and simulation parameters is given in Tab. 2.1.

At a first stage, each UE is assumed to provide PMI and CQI feedback under the assumption of perfect, ideal multi-cell channel estimation. The UEs are assumed to be equipped with multiple antennas. These antennas will be used for Minimum Mean Square Error (MMSE) receive combining, where each user only uses the channel knowledge from its serving cell, and OC with full CSI at the receiver for optimal linear Interference Rejection Combining (IRC). Based on the channel coefficients, we generate post-equalization SINRs per user and time, frequency and spatial resource.

The handover, i.e. cell assignment process is performed on the center 1.08 MHz band, where based on the current LTE specification Primary Synchronization Signal (PSS) are transmitted. These symbols provide a good received power measure, i.e. Reference Signal Received Power (RSRP), for a variety of sectors. For each BS, the scheduler groups the users to the time, frequency and spatial resources.

### 2.1.7 Initial Results and Discussion

Within the first phase, we planned to extend the typical system level simulations by introducing real measured channel coefficients. Therefore, we had to improve

<sup>1</sup><http://www.kathrein-scala.com/catalog/80010541.pdf>

Table 2.1: Simulation assumptions.

| Parameter           | Value   |
|---------------------|---|
| Channel model       | According to 3GPP SCME [10]   |
| Simulation type     | Monte Carlo plus time evolution   |
| Drops               | 500   |
| Channel evolution   | 500 ms with 1 ms resolution   |
| Scenario            | Urban-macro   |
| Propagation         | NLOS  |
| Large-scale fading  | Geo-correlated parameters maps  |
| Traffic model       | Full buffer   |
| $f_c$               | 2.6 GHz   |
| Velocity            | 3 km/h  |
| Frequency reuse     | 1   |
| Signal bandwidth    | 18 MHz, 100 RBs   |
| Inter-site distance | 500m  |
| Number of BSs       | 19 having 3 sectors each  |
| $N_t$ ; spacing     | 4 ; 4 $\lambda$   |
| Transmit power      | 46 dBm  |
| Transmit antenna    | Azimuth: FWHM of 58°<br>Elevation: FWHM of 6.2°<br>10° electrical downtilt    |
| BS height           | 32m   |
| Beamforming         | LTE vs. ZF constraint   |
| $N_r$ ; spacing     | 2 ; $\lambda/2$   |
| UE height           | 2m  |
| Feedback            | CQI and PMI<br>later full Channel State Information at the Transmitter (CSIT) |
| Feedback interval   | 6 ms  |
| Feedback delay      | 5 ms  |
| Receive processing  | MMSE or OC  |
| Channel prediction  | optional  |

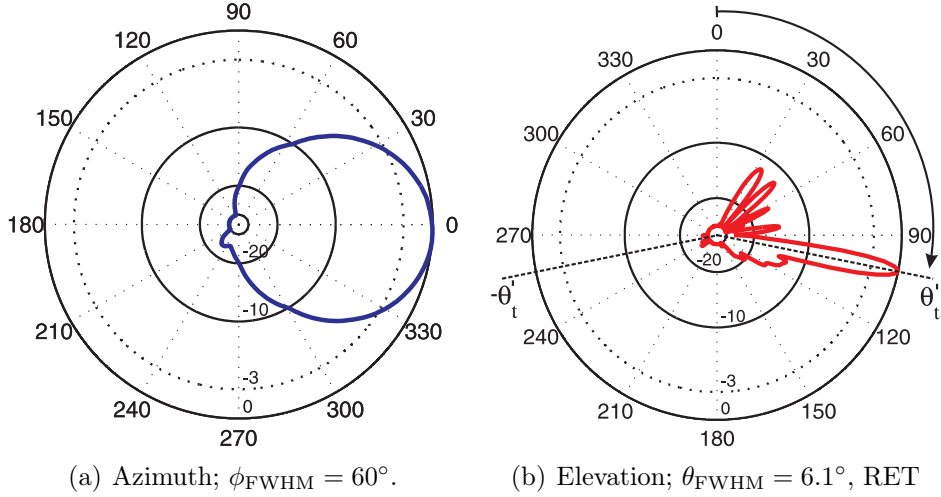


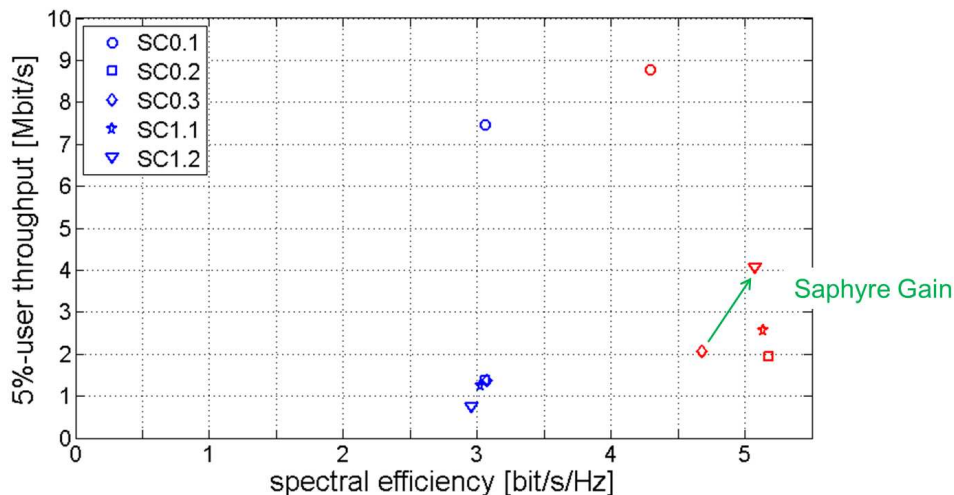
Figure 2.4: Radiation patterns from KATHREIN 80010541 antenna and 2.6 GHz carrier frequency

the common spatial channel modeling approach as described in Section 2.1.6. Due to that fact, we focus on system level evaluations, while considering the first and very simple scenario of two operators sharing the same locations of BSs, refer to Section 2.1.3. Hence, we split the scenario of co-located transmitters into the setup without spectrum sharing, where each operator uses its own dedicated spectrum of 10 MHz bandwidth. We denote this case as *SC0.x*, where *x* stands for specific subsets of configurations:

- SC0.1 = Operator A: 10 MHz and 2 UEs
- SC0.2 = Operator B: 10 MHz and 10 UEs
- SC0.3 = Operator A: 10 MHz and 2 UEs and Operator B: 10 MHz and 10 UEs

It is obvious, that the first two scenarios are very unbalanced in terms of system's traffic load. Since we consider full buffer traffic per user, both operators A and B occupy all their resources. However, the system's spectral efficiency is much higher for operator B, while the per user throughput is significantly better for UEs in the spectrum of operator A. This behavior can be seen in figure 2.5 for the case of rank 1 and rank 2 transmission. Where in case of rank 2, each BS serves 2 different users in MU-MIMO transmission mode. For reference purpose, we combine the user rates of operator A and B and determine the average spectral efficiency per sector and the 5%-ile user throughput, denoted as SC0.3.

Finally, we consider the case where both operators can jointly occupy the total 20 MHz bandwidth. Since we rely limited feedback assumptions, i.e. CQI and PMI feedback, we further assume a joint scheduling entity which decides for the user scheduling on the total 20 MHz spectrum. Since BSs are co-located it will not make sense to increase the amount of active data streams. Thus, we consider again rank 1 and rank 2 transmission. We denote this case as *SC1.x*:



For rank 1, there is hardly any gain due to spectrum and RAN sharing.

For rank 2, there is a significant gain in asymmetrically loaded system (SC1.2).

Figure 2.5: Results for co-located BSs, where spectrum sharing can be beneficial when cell load differs.

- SC1.1 = Operator A: 10 MHz and 10 UEs and Operator B: 10 MHz and 10 UEs
- SC1.2 = Operator A: 10 MHz and 2 UEs and Operator B: 10 MHz and 10 UEs

In this case of full spectrum sharing, we always consider the combined system performance, i.e. the overall median spectral efficiency per sector and the 5%-ile user throughput.

From the co-located scenario we learned that spectrum sharing pays out when the different operator’s infrastructure is asymmetrically loaded. This can be either in terms of data traffic requirements or amount of available users per cell. In the case of symmetric user and bandwidth conditions, e.g. 10 UEs and 10 MHz bandwidth for both operators, frequency selective scheduling (spectrum sharing) for 20 UEs at 20 MHz bandwidth cannot improve the system performance. Note, frequency diversity is already utilized in the non-shared scenario.

In practice, user distributions and traffic requirements will be very heterogeneous and thus the considered spectrum sharing case is highly recommended.

Within the next steps of the project, we will consider the case of distributed BS locations for two different operators as well as the use of CSI at the transmitter side for the purpose of improved precoding, e.g. under zero-forcing constraint. Furthermore, we plan to verify the channel characteristics of the used channel model. This will be done in terms of comparing user geometries obtained from emulated and measured channels and certain scenario performance indicators from Section 2.1.3.

## 2.2 Relaying and Beamforming

A quasi-static (or snap-shot) simulator using MATLAB is developed. In SAPHYRE this kind of simulator is suited to investigate advanced physical layer signal processing techniques such as transmit beamforming or complicated receiver concept. It is also suitable for system function such as fast adaptive resource scheduling.

### Scenario Description

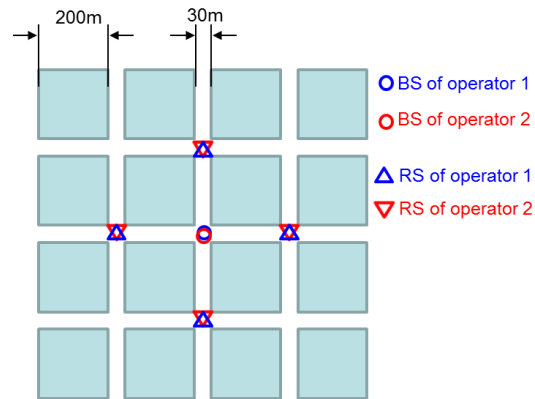


Figure 2.6: The Manhattan grid with a single cell-layout.

The initial test scenario for this simulator is the wireless backhaul scenario with relays in Figure 2.6. Due to strong shadowing effects in the network, dense networks are required to guarantee the Quality of Service (QoS) at the user terminals. To this end, each cell in the Manhattan grid comprises of one BS and four relays such that the coverage holes are avoided and the QoS of the User Terminals (UTs) are improved. The two operators who operate in the same area have the overlapped layout. More precisely, both the BSs and relays of the two operators are close to each other.

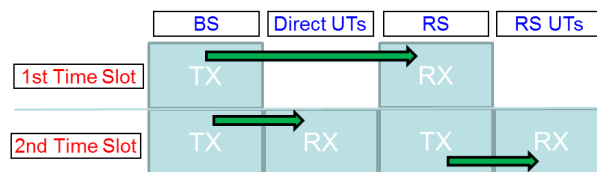


Figure 2.7: Timing in the two-hop networks. Direct UTs are users that are directly served by the BS while RS UTs are served by the RSs.

We define two types of users in this network. Direct users are directly served by the BS while the Relay users are served by the relay. Whether a user is a direct UT or a Relay UT in our initial setup is simply decided by the measured Received Signal Strength Indicator (RSSI) from BS and RS. The relays employed here are

one-way Decode-and-Forward (DF) MIMO relays. As shown in Figure 2.7, in the first time slot, the data of the relay users is sent via the wireless backhaul link between the BS and the relay. There is no direct link between the BSs and the RS UTs due to the pure channel quality. Then the relay demodulates and decodes the data and then encodes and modulates it again before transmitting to the users. In the second time slot, the BS transmits to its direct users while the relay transmits to the RS UTs. It is assumed that in the second time slot the communication from the BS to direct users and that from the relay to RS users use orthogonal resources, e.g., different subcarriers. Thus, there is no interference created between the direct UTs and the RS UTs. Furthermore, we assume the transmission between the BS and the RS is error-free. Note that the functionality of the relay here is similar to the Layer 3 relay which is defined in LTE Rel. 10, i.e., the relay acts as a Pico BS and it is recognized as a BS from the viewpoint of the UTs. The key simulation parameters are given in Table 2.2

Table 2.2: Key simulation parameters.

| Parameter                       | Value                                |
|---------------------------------|--------------------------------------|
| Carrier frequency               | 2 GHz                                |
| Channel model                   | WINNER II B1 NLOS [18]               |
| Traffic model                   | Statistics with full-buffer downlink |
| eNB location/height             | 15 m (above rooftop)                 |
| eNB number of sectors           | 4                                    |
| eNB antennas per sector         | 2                                    |
| eNB maximum Tx power per sector | 46 dBm                               |
| eNB elevation+antenna gain      | 14 dBi                               |
| eNB noise figure                | 5 dB                                 |
| RN location/height              | 10 m (below rooftop)                 |
| RN antennas                     | 4 (omnidirectional)                  |
| RN maximum Tx power             | 24 dBm                               |
| RN elevation+antenna gain       | 9 dBi                                |
| RN noise figure                 | 7 dB                                 |
| UE location/height              | 1.5 m (above rooftop)                |
| UE antennas                     | 1 (omnidirectional)                  |
| UE elevation+antenna gain       | 0 dBi                                |
| UE noise figure                 | 7 dB                                 |

### Mobility model

In this scenario the user movement is modeled using the Pathway Mobility model. This restricts the user movement to predefined paths in the case of the Manhattan Grid the streets between the buildings. In the beginning, the direction of a user moving through the street is chosen randomly. At a crossing, a user keeps straight

on with a certain probability  $P_{\text{straight}} = 0.5$ . The turn probability is the same for both directions and can be calculated as  $P_{\text{turn}} = (1 - P_{\text{straight}})/2$ .

## Traffic model

Table 2.3: Considered service classes, usage probabilities and QoS requirements for service classes in the implemented traffic model

| Parameter      | VoIP      | Audio     | Video     | FTP       | HTTP      |
|----------------|-----------|-----------|-----------|-----------|-----------|
| $Prob[\%]$     | 39.6      | 6.1       | 16.9      | 13.3      | 24.1      |
| $BER$          | $10^{-6}$ | $10^{-6}$ | $10^{-6}$ | $10^{-6}$ | $10^{-6}$ |
| $R[Kbps]$      | 64        | 128       | 5000      | 2000      | 512       |
| $\Delta_p[ms]$ | 100       | 100       | 200       | 200       | 200       |

Since MATLAB is not very suitable for modeling protocols, to model the traffic characteristics (requirements, session duration) we use statistics on MAC-SAP. To this end, we specify three parameters for each user as QoS requirements, namely the bit error rate (BER), the data rate ( $R$ ), and the maximum packet delay ( $\Delta_p$ ). These requirements depend on the service the user requests (e.g. Voice over IP (VoIP), video streaming). To assign different services to the users, we apply a traffic model for metropolitan areas as described in [17]. There, according to certain probabilities, the users are divided into different service classes. In contrast to the model in [17], we restrict the investigations to the five most probable service classes. The used service classes, their probabilities and their requirements are listed in Table 2.3. The time a user requires a specific service, the so called session duration, is randomly chosen from a certain distribution which differs for each service class [17].

## User scheduling

Three user scheduling methods are implemented for the simulation. That is, sum rate maximization, round robin or proportional fair scheduling are employed in each snap-shot or channel realization.

## Link to system level interface

To evaluate the spectral efficiency, the bit level procedures are mapped using a mutual information based link to system level interface [19]. The mapping curve is shown in Figure 2.8, where the Shannon capacity is also plotted as a reference. Note that the SINR operating region is between -3 dB (below which communication is not possible) and +17 dB (above which the UTs cannot make use of any additional signal power).

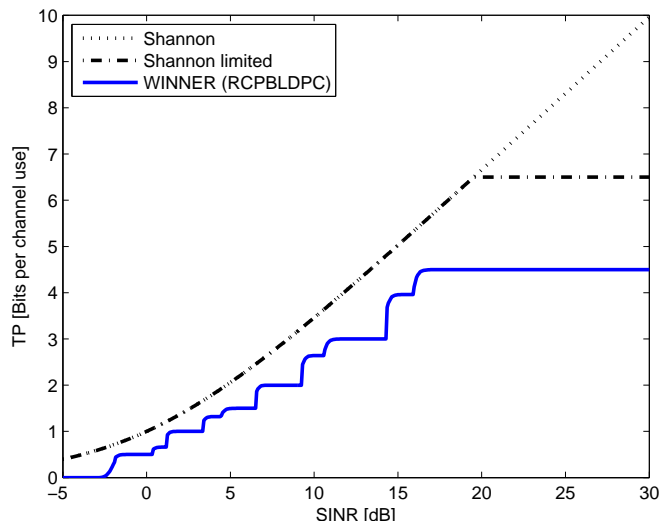


Figure 2.8: Link to system mapping for the rate-compatible punctured block low density parity check codes, considering 10 combinations of modulation size and code rate (1/3 to 4/5. BPSK to 64-QAM).

## 2.3 Network Layout, Propagation Environment, and Traffic Characteristics

This section describes key modeling aspects developed by partner TNO. In particular, we discuss approaches of modeling network layout (for both homogeneous and heterogeneous deployments), propagation modeling taking into account large-scale fading (e.g. distance-based path loss, shadowing, etc.), and traffic modeling (either uniformly or non-uniformly distributed).

### 2.3.1 Network layout

Two types of networks are considered in the study: macro-cellular networks and a network of hotspot cells. The former is applicable for all the sharing scenarios considered in the study, while the latter is only used in sharing scenarios with heterogeneous deployments where a macro-cellular network of one operator overlays with a network of hotspot cells of another operator. Each network is characterized by its ownership, Radio Access Technology (RAT) (HSPA or LTE), carrier, bandwidth, site locations, and BS parameters. Each macro-cellular network involved in the sharing scenarios comprises twelve sectorized (12x3) sites that are organized in a hexagonal layout with a tunable inter-Site Distance (ISD), as depicted in Figure 2.9. A wraparound technique is applied to mimic infinite networks and avoid boundary effects. As also depicted in Figure 2.9, the considered macro-cellular networks may have different degrees of co-siting and “co-azimuthing”, denoted  $\Delta_{CS}$  and  $\Delta_{CA}$ , respectively, and defined in the figure. Note that  $\Delta_{CS} = \Delta_{CA} = 0$  corresponds with a scenario of fully co-sited and -azimuthed networks.

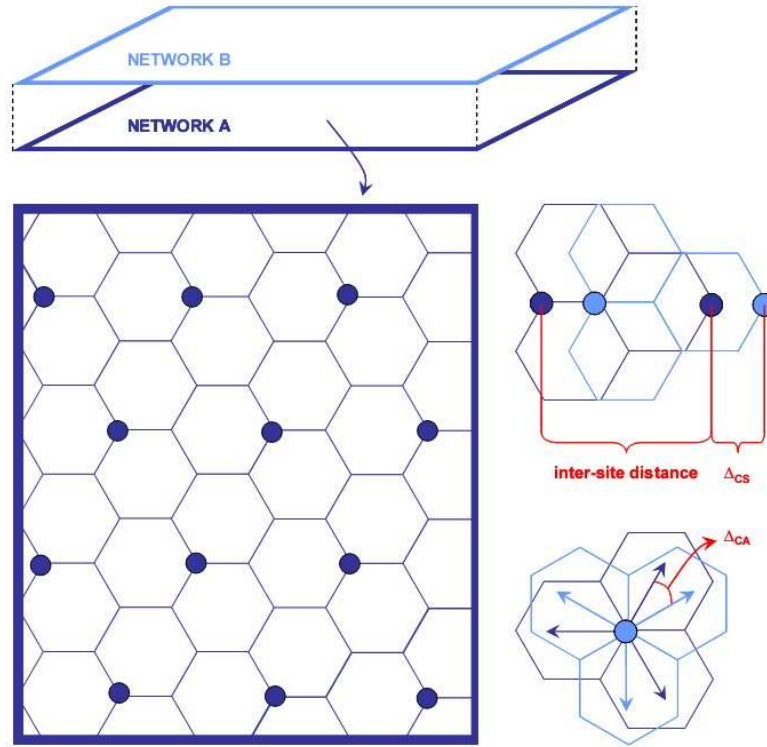


Figure 2.9: Network layout

In heterogeneous scenarios, it is assumed that there are a certain number (denoted  $n$ ) of hot-spot cells (of Operator A) evenly located within the (hexagonal) coverage area of each macro-cell (of Operator B). It is further assumed that Operator B “owns” all the subscribers, although all the terminals have also right to access the hot-spot cells and their spectrum based on agreement between the two operators. Figure 2.10 shows the relative locations of hot-spot cells with regard to the coverage area of a macro cell for  $n= 1, 3, 6$  and  $12$ , respectively.

### Propagation Models

The propagation environment is mainly characterized by distance-based path loss, shadowing and indoor penetration loss. A Hata-Okumura or COST 231 Hata model is used to model the distance-based path loss, with the possibility of choosing environment-specific parameters, e.g. the environment (large cities, small-to-medium cities, sub-urban or rural area), base station and terminal heights, etc. The directional macro-cell antennas have an antenna pattern given by 3GPP TR36.942 [1] with an effective main lobe antenna gain of 11.5 dBi (corrected for slant/cable loss) and maximum transmit power of 46 dBm, while each hot-spot cell has an omni-directional antenna with maximum transmit power of 30 dBm. The correlation between shadowing to cells controlled by the same and different sites is considered. The key propagation parameters, assuming carrier frequency of 2100 MHz, base station height of 30 meter and terminal height of 1.5 meter, are summarized in Table 2.4. Multipath fading is not considered.

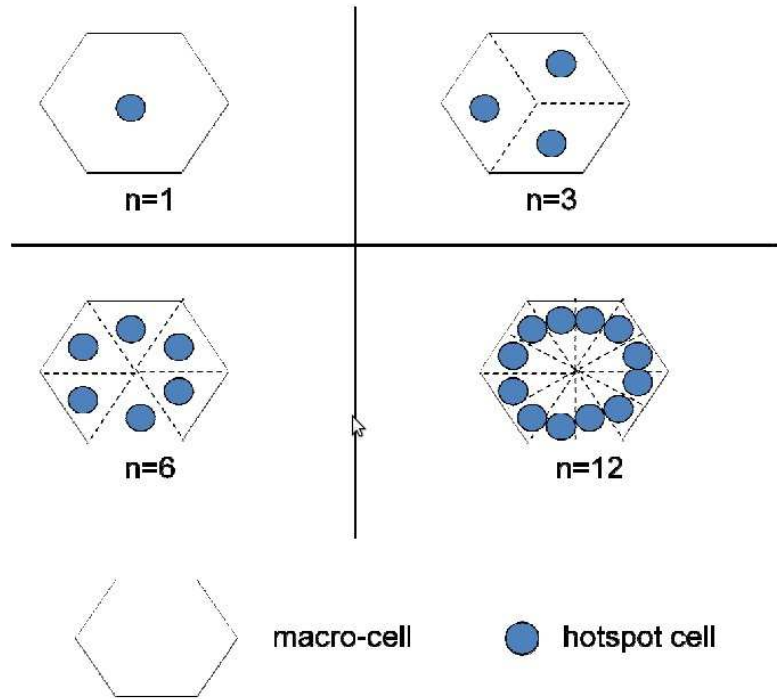


Figure 2.10: Number of hotspot cells and their relative locations.

|   |                                   |            |
|---|-----------------------------------|------------|
| Main lobe antenna gain after cable/slant loss | 11.5                              | <u>dBi</u> |
| Maximum transmit power (macro cell)           | 46.0                              | <u>dBm</u> |
| Maximum transmit power (hotspot cell)         | 30                                | <u>dBm</u> |
| Noise power density (per PRB)                 | 121.5                             | <u>dBm</u> |
| Noise figure                                  | 8.0                               | <u>dB</u>  |
| Carrier frequency                             | 2100                              | <u>MHz</u> |
| Path loss (macro cell)                        | $138.5 + 32.23 \log_{10}(d_{km})$ | <u>dB</u>  |
| Path loss (hotspot cell)                      | $127 + 30 \log_{10}(d_{km})$      | <u>dB</u>  |
| Shadowing standard deviation                  | 8.0                               | <u>dB</u>  |
| Intra-site shadowing correlation              | 1.0                               |            |
| Inter-site shadowing correlation              | 0.5                               |            |
| Indoor penetration loss                       | 17.0                              | <u>dB</u>  |

Table 2.4: Key propagation parameters.

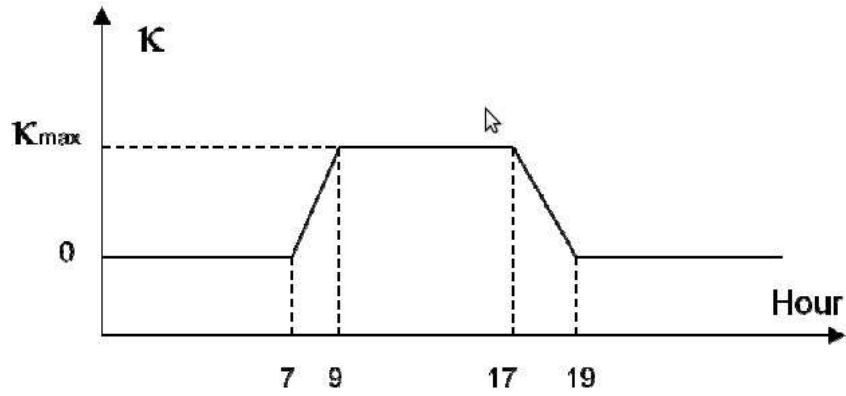


Figure 2.11: Daily profile of location-dependent traffic distributions.

### Traffic Model

Traffic flows are modeled as the download of file with a lognormally distributed size with mean 1.0 Mb and a standard deviation of 1.5 Mb. Flows are generated according to a Poisson process with average arrival rate  $\lambda$ . Either a fixed value of  $\lambda$  or a daily traffic profile with varying values of  $\lambda$  may be applied, depending on the simulation scenario. The generated flows are assigned to one of the sharing operators/networks according to the assumed market shares of the operators. For example, if the market shares of Operator A and Operator B are 75% and 25%, respectively, 75% (25%) of the generated flows are assigned to Operator A (Operator B). Note that, in scenarios with heterogeneous deployments all the subscribers belong to Operator B. For scenarios with homogeneous deployments (two overlaying macro-cellular networks), generated traffic flows are assumed to be uniformly distributed in the spatial domain. While for scenarios with heterogeneous deployments (a macro-cellular network overlaying a network of hot-spot cells), generated traffic flows are assumed to be location-specific to certain extent: with probability  $\kappa$ , the location of a generated flow is sampled in the service area of the hotspots, while with probability  $1-\kappa$  it is sampled uniformly over the entire coverage area. In order to model the migration of subscribers between e.g. residential and commercial area,  $\kappa$  may vary during a day. Figure 3 shows an example of daily profile of  $\kappa$ , where the maximum value of  $\kappa$  is denoted as  $\kappa_{\max}$ .

At the arrival of each flow, its location, subscription (which operator it belongs to), path loss, shadowing, and (download) file size are sampled following the distribution as discussed above. For each initiated flow, the serving cell is selected based on the received pilot strength. At any time, the available radio resources in each cell are evenly shared by the served flows. Once a download is completed, the corresponding flow disappears from the system.

### Other Aspects

Spectrum and/or infrastructure sharing is executed at a certain time scale (seconds or above), according to a window-averaged metric, e.g. cell-specific traffic loads

(applying a certain averaging window) served by individual networks. In the applied spectrum sharing scheme, spectrum is assigned to the different networks with a certain granularity. The following default settings are assumed for the corresponding parameters:

- Spectrum and/or infrastructure sharing time scale: 60 seconds
- Load-averaging window length: 60 seconds
- Granularity of spectrum sharing: 6 PRBs.

### 2.3.2 Performance Metrics Definition

For an adequate assessment of the algorithms that are developed, a clear set of performance metrics is necessary to assess the gains and costs of spectrum and/or infrastructure sharing, to compare different sharing algorithms from different perspectives and state their practical usability. The following aspects should be taken into account:

- Signalling overhead: the amount of additional side-information exchanged between operator's entities has to be quantified and should be acceptable when compared to the gains.
- Complexity: including number and type of operations that have to be performed, additional components and interfaces that have to be defined and time needed to obtain optimum allocation.
- Gains: compare the developed/proposed sharing scenarios and algorithm to reference scenarios as well as with other sharing algorithms, and observe where and what are the gains: spectral efficiency, energy savings, network capacity, end-user performance (average throughput, cell edge throughput, X-percentile user throughput).
- Fairness: the algorithm development should take into account service differentiation, and competition between operators. The distribution of radio resources should also take into account inter-operator and inter-user fairness. The importance of inter-operator fairness depends on the defined policy (prioritization) among sharing operators. If monetary compensation is part of the policy, the relative amount of resources utilised and/or performance experienced by customers of different operators should be monitored, in order to allow comparison with brought in resources and/or monetary compensation schemes.
- Other performance indicators: the following extra performance indicators are monitored to ensure that sharing will not introduce unacceptable performance degradation: no-coverage probability (overall and per hour), call blocking probability (overall and per hour), resource utilization.

### *2.3 Network Layout, Propagation Environment, and Traffic Characteristics*

In the system-level simulation we have performed so far, only part of the performance metrics are among the direct output of the simulations, e.g. network capacity, end-user performance, no-coverage/call-blocking probabilities, and resource utilization. Others are mainly addressed qualitatively or based on analytical analysis.



## 3 System Level Evaluation

In order to verify the sharing concepts developed in SAPHYRE, dynamic, advanced and RAT specific system level simulators are used. An overview of the methodologies is given in the following.

### 3.1 Multi-Operator Multi-Cell Simulation Based on NS3

CFR decided to use the Network Simulator-3 (NS3) [8] tool to run its simulations and validate the proposed resource allocation algorithms. Thus, a first important contribution was the extension of the tool itself to make it support multicell scenarios and resource sharing among network operators. In particular, since CFR has been mainly focusing on spectrum sharing instead of infrastructure sharing, the simulation software has been extended only to add that capability. Further modifications for the introduction of infrastructure sharing are only planned up to now.

#### 3.1.1 Tool description

The Network Simulator-3 (NS3) is a very well known tool widely used in the research community for the simulation of heterogeneous communication networks. It is an event-driven asynchronous simulator entirely open source, free and managed by an active community of developers. The whole TCP/IP protocol stack is implemented, with the most important protocols at the transport, network, and datalink layers (e.g. TCP, UDP, IP, ARP, IEEE 802.11, IEEE 802.16). Several types of applications are provided with the basic version of the code (e.g. CBR, VBR) and many others can be implemented just by extending the base classes. The transmission channel is implemented as well, both wired and wireless. The level of detail in the channel definition is not extremely deep (e.g. no symbol-level operations), even though it has been definitely improved with respect to the previous version of the software, ns-2. The code includes as well built-in data structures and functions to deal with several types of networks, from sensors to satellite communications.

Besides its great flexibility, one of the main features of this simulator is the modularity. The implementation is not monolithic at all and this makes its extension simpler. This is particularly appealing for our purposes, since the analysis of spectrum sharing, while involving physical and datalink layers, implies important consequences in protocol design at higher layers as well, thus being an inherently cross-layer problem. These reasons motivate our choice to employ NS3 as the system level simulator for the SAPHYRE project. The extended version proposed in [21] was considered because of its capability to support the Long Term Evolution (LTE) of the Universal Mobile Telecommunications System (UMTS) [2]. It is possible to create Base Stations (called eNodeBs, or Evolved Node Bs (eNBs))

and user terminals (called UEs) which can communicate with the eNBs. Most of the functionalities of the physical channel and medium access were implemented, while some of them were still empty or a sample code was provided, thus giving the programmer the opportunity to introduce and test new algorithms. This is the starting point of the implementation and validation work done by CFR. The main contribution in this direction was the introduction of a novel software extension of this NS3 version to characterise spectrum sharing scenarios where cooperation is established among multiple operators, each with a considerable number of nodes. To this aim, original software structures were introduced. First of all, the support to multi-cell multi-operator networks with overlapping spectra in the downlink was provided. Then, a class describing a virtual *frequency market* was inserted in the simulator structure. This class implements the functionalities of a virtual arbitrator, and does not represent a physical entity of the network, but rather it determines the sharing policy of the frequencies belonging to the common pool. In other words, its role is to abstract the set of rules agreed by the operators when determining the shared portion of the spectrum. Two main sharing meta-policies can be identified, namely *orthogonal* and *non-orthogonal*. In the former case, the frequencies of the shared pool still remain into exclusive usage of exactly one operator, although not necessarily the one that detains the legal property of the access on that frequency. In the latter, also simultaneous access on the same frequency is possible. In both cases, the arbitrator structure is required to give an abstract representation of every other sharing policy detail, such as priority rules among the operators in case of conflicting assignments. CFR focused on orthogonal sharing, which is immediate to describe and does not require to detail any power control policy for shared frequencies. However, the extension to the non-orthogonal case is under development. Some sharing policies were implemented and tested, and the respective results are discussed in the following sections. With reference to the software modifications, more details are given in [13].

#### 3.1.2 System model

The reference systems of our study are OFDMA networks, in particular those compliant with the LTE standard [2]. As seen before, when discussing spectrum sharing policies it is important to clarify the orthogonality of the access scheme in the pool of common frequencies, where “orthogonality” means “impossibility of simultaneous usage by more than one operator.” The non-orthogonal approach requires the description of a power control mechanism for the involved entities (i.e. the eNBs); we will limit the following discussion to the orthogonal sharing case. Therefore, from this point on, we will assume that eNBs share orthogonally the pool of common frequencies so that each frequency resource can be assigned to at most a single operator (which, in turn, will use it for one of its UEs) within an allocation time slot. We consider a short time-scale spectrum sharing, with the inter-operator trading of the resources is done on a fine-grained basis, in our case corresponding to the LTE subframe duration, i.e. 1 ms.

The proposed framework can be divided into three parts. First of all, the spectrum usage parameters must be provided, i.e. physical details such as the transmission

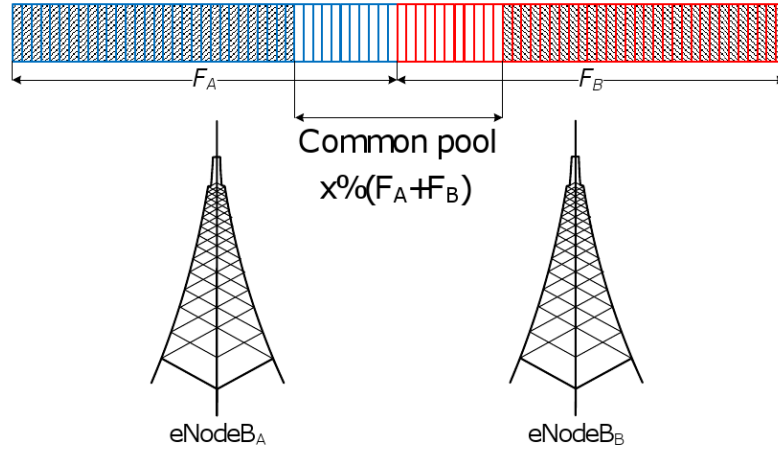


Figure 3.1: Spectrum sharing

frequency, the channel bandwidth, the sharing percentage, and so forth. Then, local scheduling and resource allocation algorithms must be executed by each eNB in order to generate an allocation map that represents the proposed serving scheme in its cell (i.e. the association  $\langle \text{AT}, \text{UE} \rangle$ ). Finally, a virtual market is in charge of collecting the local allocation maps and derive the serving schemes that must be adopted by each eNB, according to the chosen contention solving policy.

### Spectrum management

Once the physical parameters have been determined, the network operators select the set of frequencies on which they plan to interoperate. The policy behind such a cooperation agreement is more related to the economic agreement between the operators and their business models. However, along with different allocation and coordination techniques, it represents an interesting research topic and, through system level simulations it is possible to evaluate quantitatively several sharing approaches. Figure 3.1 shows the scheme adopted to define the system sharing capabilities. According to the selected bandwidth percentage to be shared, the eNBs (each one managed by a different operator) will allow partial access to UEs belonging to other domains. The choice to consider adjacent spectra for the eNBs is not restrictive and has been introduced just for simplicity.

### Intra-cell allocation

The cell capabilities are fully characterised when the physical components have been defined. Then, a joint scheduling and resource allocation algorithm is needed to design a proper downlink transmission scheme. The definition and the analysis of efficient schemes are not directly investigated here. However, the architecture of the simulator here considered makes it simple to plug-in any of such algorithms and

validate their performance. An example is given in [12].

For what concerns the scope of this discussion, two basic algorithms have been implemented and compared. On one hand, *max throughput* represents an allocation scheme for which the resources are always allocated to the best UEs, without taking into account fairness among users. On the other hand, a fair approach is proposed, denominated *fairness*, where the available system resources are distributed among the users in a Round Robin way, thus lowering the overall throughput but increasing the average level of service of each UE. Figure 3.2 depicts a sample scenario, where 10 UEs and 10 resources, hereinafter referred as allocation tile (ATs), are considered. For the particular case of LTE networks, each AT lasts 1 ms and spans in frequency for 12 subcarriers. By selecting the first approach, i.e. *max throughput*, all the available resources are allocated to the UEs with the best channel quality indicator (CQI) that will be discussed in Section 3.1.3). Thus, by exploiting multiuser diversity, the system throughput can be very high. However, UEs with lower CQIs will never be served. Therefore, an additional technique has been introduced, i.e. the *fairness* mechanism which, as visible in the figure, will provide service to all the registered UEs. As in the previous case, each AT is allocated to the best UE, but each user will be given at least a certain amount of resources thus preventing starvation. In particular, the distribution of the ATs happens in a Round Robin way with the pooling starting from the UEs with the best CQI and moving to those in a worse condition. During the first allocation round, each UE is given

$$TH_{min} = \left\lfloor \frac{N_{AT}}{N_{UE}} \right\rfloor, \quad (3.1)$$

where  $N_{AT}$  and  $N_{UE}$  are respectively the total number of ATs and of registered UEs in the cell. Then, once that this minimum threshold has been guaranteed to all the users, all the remaining ATs are distributed again with a Round Robin policy by assigning one AT per UE starting first from those with better channel conditions. In the proposed example, the threshold in equation (3.1) is equal to one, so all the UEs will be allocated a single AT.

#### Inter-cell coordination

The sharing contention policy is implemented in a separate module, here called *virtual market*. The relevant class (we refer to an Object-Oriented Programming, or OOP, paradigm) implements an arbitration rule which defines how the operators bargain the access to the common portion of the spectrum. Any complex strategy can be implemented within this class, possibly involving further extensions. In particular, this may be the place where to implement, in an entirely modular manner, some procedures inspired by game theoretic principles.

Each eNB, after generating its own allocation map, sends it to the *virtual market* who gathers all the cells' allocation information and rearranges the allocation map according to the sharing policy. For the validation phase we propose immediate implementations of scheduling and resource allocation algorithms, as well as a simple procedure to handle the contentions among operators. Each eNB is assigned a

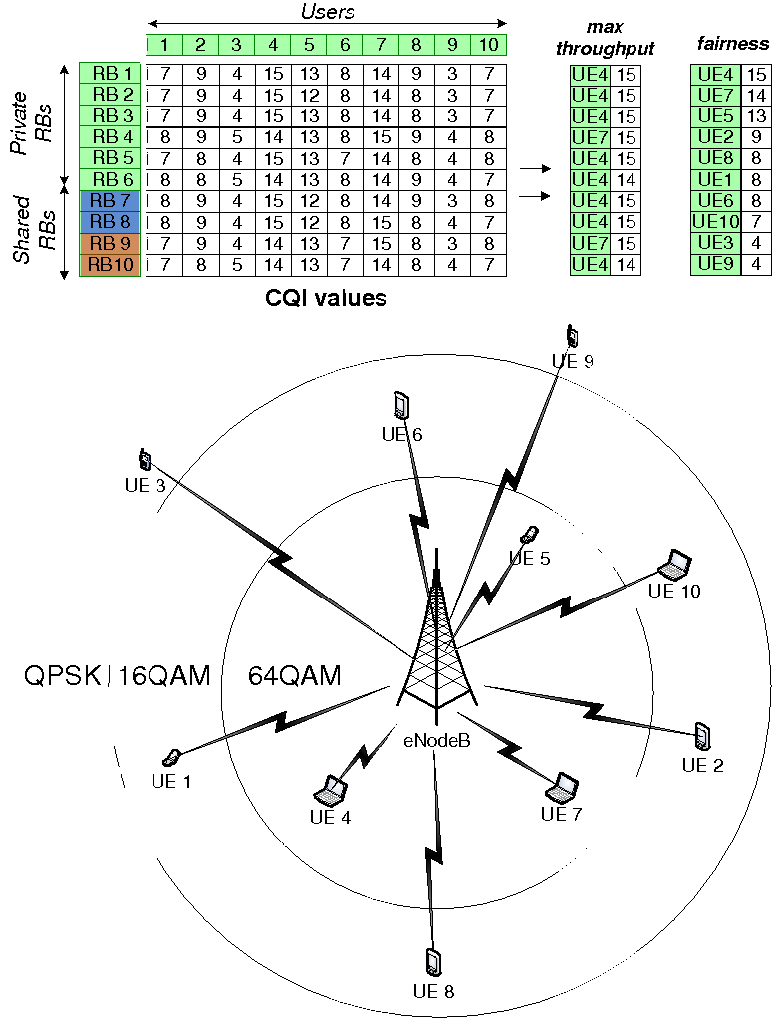


Figure 3.2: Intra-cell allocation

*priority* value per frequency subchannel, defined as

$$PR_{eNB_j, AT_{pool,i}} = \begin{cases} p, & AT_{pool,i} \in F_{eNB_j} \\ 1 - p, & \text{otherwise} \end{cases}, \quad (3.2)$$

where  $j \in \{1, \dots, m\}$  represents the eNB identifier,  $m$  is the total number of eNBs involved in the sharing process,  $p \in [0, 1]$  is the priority level given to the eNB,  $F_{eNB_j} = \{AT_{j,1}, \dots, AT_{j,n_j}\}$ ,  $n_j$  is the total number of ATs available at eNB $_j$ , and  $AT_{pool,i} \in F_{eNB_j} \cup \dots \cup F_{eNB_m}$ . In other words, shared resources are assigned based on these priority levels; obviously, the UEs associated to eNB $_j$  will always have higher priority than all other competing users. The proposed approach can be made even simpler if we assume  $p = 1$  and  $m = 2$ : an eNB will assign to its UEs the shared resources belonging to the *competitor* eNB, referred to as eNB $_c$ , only if these are not allocated to UEs belonging to eNB $_c$ . Therefore, when multiple players request the same resource, only the one with the highest priority will get it. The others end up with no assignment, which is in general inefficient.

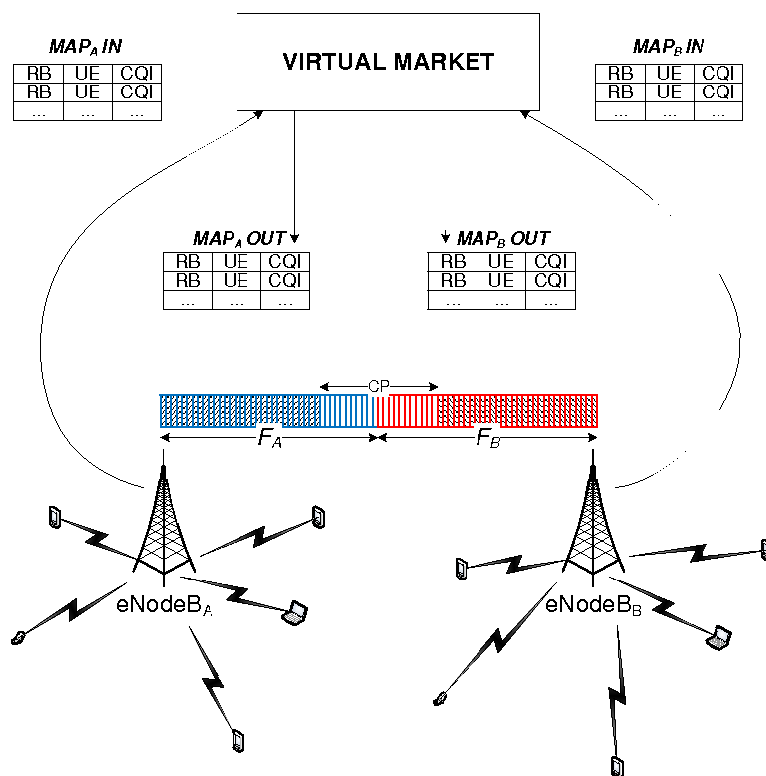


Figure 3.3: Inter-cell coordination

We stress that this general strategy is not given as an optimal allocation, which ought to be derived from a (game) theoretic perspective. Other WPs and tasks of the SAPHYRE project are demanded to study the problem. Rather, such an intentionally non-optimised (and actually inefficient) policy serves to show the effectiveness of our software implementation. Moreover, it can be thought of as a characterisation of the inefficient Nash equilibria in the games with *competitive* sharing, while the goal of spectrum sharing should rather be a *collaborative* assignment of frequencies. Thus, our reference allocation policy correctly reflects that, if the whole common pool is shared competitively, in the long run only inefficient and unfair allocations will be achieved. However, we also remark that more efficient solutions derived through game theory, either available in the literature or originally developed, can be tested and validated within the modular framework proposed, so as to determine the choice that better suits the operator needs.

### 3.1.3 Simulation scenario

In order to test the software architecture that we have implemented, we have run some simulations. The algorithms used are meant to be just an example to show how things work, so they are not expected to be the optimal solution. We are more interested in the performance and the usability of the simulator itself. In

the following we present the results of a simulation campaign conducted with the extended framework for spectrum sharing in NS3.

The scenario consists of two co-located eNBs, both with a coverage of 1500 m. An increasing number of UEs, characterised by low mobility, are registered to each station, and are uniformly distributed within the associated eNB coverage area. Each user is supposed to be always backlogged and so the network operates in saturation conditions.

As already mentioned, each user perceives a different quality of the channel according to its position and to radio propagation effects (e.g. shadow and multipath fading). An ideal uplink channel is established between each UE and the corresponding eNB, used for the transmission of the CQIs associated to each AT. In fact, thanks to this information, the eNB can select an adequate MCS. As reported in Table 3.1, LTE technology provides 15 different option schemes [3], where ECR stands for Effective Code Rate and represents the robustness of the selected coding scheme. Hence, the MCS determines the quantity of bits that can be actually transmitted in an AT. The main simulation parameters are provided in Table 3.2.

| CQI | Modulation | ECR    | Spectral Efficiency |
|-----|------------|--------|---------------------|
| 1   | QPSK       | 0.0762 | 0.15                |
| 2   | QPSK       | 0.1172 | 0.23                |
| 3   | QPSK       | 0.1885 | 0.38                |
| 4   | QPSK       | 0.3008 | 0.6                 |
| 5   | QPSK       | 0.4385 | 0.88                |
| 6   | QPSK       | 0.5879 | 1.18                |
| 7   | 16QAM      | 0.3691 | 1.48                |
| 8   | 16QAM      | 0.4785 | 1.91                |
| 9   | 16QAM      | 0.6016 | 2.41                |
| 10  | 64QAM      | 0.4551 | 2.73                |
| 11  | 64QAM      | 0.5537 | 3.32                |
| 12  | 64QAM      | 0.6504 | 3.9                 |
| 13  | 64QAM      | 0.7539 | 4.52                |
| 14  | 64QAM      | 0.8525 | 5.12                |
| 15  | 64QAM      | 0.9258 | 5.55                |

Table 3.1: LTE Modulation and Coding Scheme

The simulation campaign is executed to investigate the reliability of the proposed framework, in terms of cell theoretical capacity, aggregate throughput, and execution time. More specifically, the performance metrics considered are:

- **Cell Sum Capacity**, which represents the sum of the Shannon capacity reached in a cell on each subchannel. It is given by

$$C = \sum_{i=1}^{N_{UE}} \sum_{j=1}^{N_{sub}} (B \cdot \log_2(1 + SINR_{ij} \cdot \delta_{ij})), \quad \delta_{ij} = \begin{cases} 1, & \text{UE}_i \text{ allocated to sub}_j \\ 0, & \text{otherwise} \end{cases} \quad (3.3)$$

where  $N_{sub}$  is the total number of subchannels that can be exploited in the downlink of the cell (i.e., including those shared by the other eNBs (eNBs)), and  $SINR_{ij}$  is the SINR at UE  $i$  on subchannel  $j$ .

- **System Throughput**, which represents the aggregation of the actual data rates delivered to each UE by using the MCSs in Table 3.1.
- **Execution time**, which represents the time required for the execution of a simulation run. We expect an increasing behaviour in the number of UEs and in the sharing percentage because of the higher computational complexity needed to perform a greater number of operations. The duration of a single run is of 10 ms. According to the Monte Carlo simulation method, 1000 runs have been executed for each parameters combination in order to have a good characterization of the channel behaviour, with each UE replaced at each repetition in order to simulate the mobility. The reference machine is a computation server with 48 Pentium CPUs, 64 GB RAM and running GNU/Linux Ubuntu 11.04 as the operating system. It must be noted that, even though the number of available processors is considerable, the NS3 software is inherently non parallel and thus all the runs were always executed on a single processor as if it were a single CPU machine. The only advantage of having more CPUs derived from the possibility to execute several simulations in parallel, one for each different combination of the input parameters (i.e. number of UEs and sharing percentage).

#### 3.1.4 Example Simulation Results

Figures 3.4–3.5 show the performance in terms of capacity and throughput achieved by each cell when the *max throughput* allocation is used. As expected, the actual throughput value is significantly below the channel capacity, which represents the theoretical limit achievable with such a channel condition. The actual amount of data transmitted depends on the ECR and is upper bounded by the Shannon capacity. However, the behaviour of both capacity and throughput as functions of the sharing percentage for different numbers of users is qualitatively similar, meaning that they differ only by a scaling factor due to the use of real coding and modulation schemes. A first conclusion that might be drawn from these figures is that, if spectrum sharing is performed in a *competitive* manner, there is no gain for the operators in sharing their frequencies. In fact, the higher the sharing percentage, the more likely the resource conflicts. Due to the lack of collaboration among the operators, they simply try to get the best frequencies, whereas other less appealing resources are wasted. This is a typical phenomenon of *non cooperative* game theory, i.e. an inefficient Nash equilibrium as a result of the selfishness of the players [20]. The situation is made worse by the constraint that the private subchannels of one eNB cannot be accessed by the other eNBs, and so some resources might be unused. These are the main reasons for which all the curves, independently by the number

| Parameter                        | Value                                  |
|----------------------------------|--|
| Centre Frequency                 | 2110 MHz                               |
| Channel Bandwidth                | 20 MHz                                 |
| Subcarrier Bandwidth             | 15 kHz                                 |
| Doppler frequency                | 60 Hz                                  |
| $AT_{bandwidth}$                 | 180 kHz                                |
| $AT_{subcarriers}$               | 12                                     |
| $AT_{OFDMsymbols}$               | 14                                     |
| eNodeB TX power per subchannel   | 26.98 dBm                              |
| Noise figure (F)                 | 2.5                                    |
| Noise spectral density ( $N_0$ ) | -174 dBm/Hz                            |
| Macroscopic pathloss             | $128.1 + (37.6 \cdot \log_{10}(R))$ dB |
| Shadow fading                    | log-normal ( $\mu = 0, \sigma = 8$ dB) |
| Multipath                        | Jakes model with 6 to 12 scatterers    |
| Wall penetration loss            | 10 dB                                  |
| Simulated interval               | 10 s                                   |
| Frame duration                   | 10 ms                                  |
| TTI                              | 1 ms                                   |

Table 3.2: Main system parameters

of UEs, are almost flat. In some runs we saw even a slight loss compared to the case of 0% sharing, but these were only few instances of the 1000 we have run (consider that the results showed have a 95% confidence interval with a maximum relative error smaller than 1%). The modularity of our software allows for a prompt insertion of efficient game theoretic strategies for inducing the operators to achieve a *collaborative* sharing, thus improving the allocation efficiency.

Another important intuition that can be gained from those figures is that both performance indices increase with the number of users. This is an effect of the increased multiuser diversity: the greater the number of UEs, the higher the probability that for each subchannel there is at least one of them with a good CQI. However, this increase is significant only when the number of users is low. When more users are in the system, the marginal improvement due to multiuser diversity becomes lower since for almost all the subchannels there is a user with good CQI. Thus, the curves seem to saturate around 18 users.

To sum up, the results validate the reliability of our model in spite of an inefficient sharing policy, which was not the scope of this simulation campaign. Thanks to the modularity introduced, the contention technique can be adapted to different needs, and in particular to pursue a cooperative sharing, where system capacity and throughput increase when the spectrum sharing percentage becomes higher.

Our framework also enables a comparative analysis among different allocation approaches. Therefore, we can compare the *max throughput* allocation with the

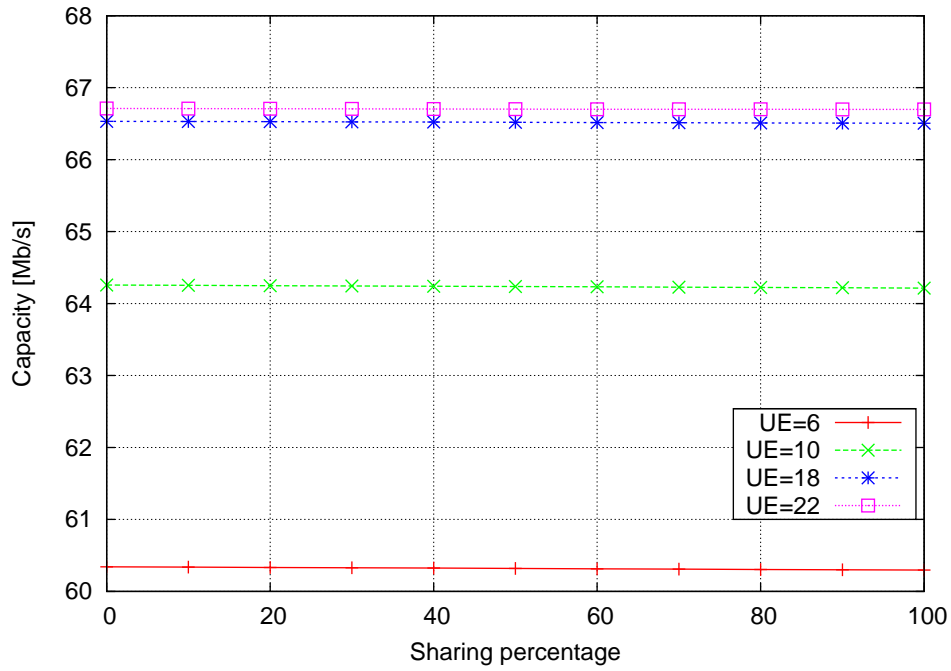


Figure 3.4: Cell capacity of the *max throughput* allocation

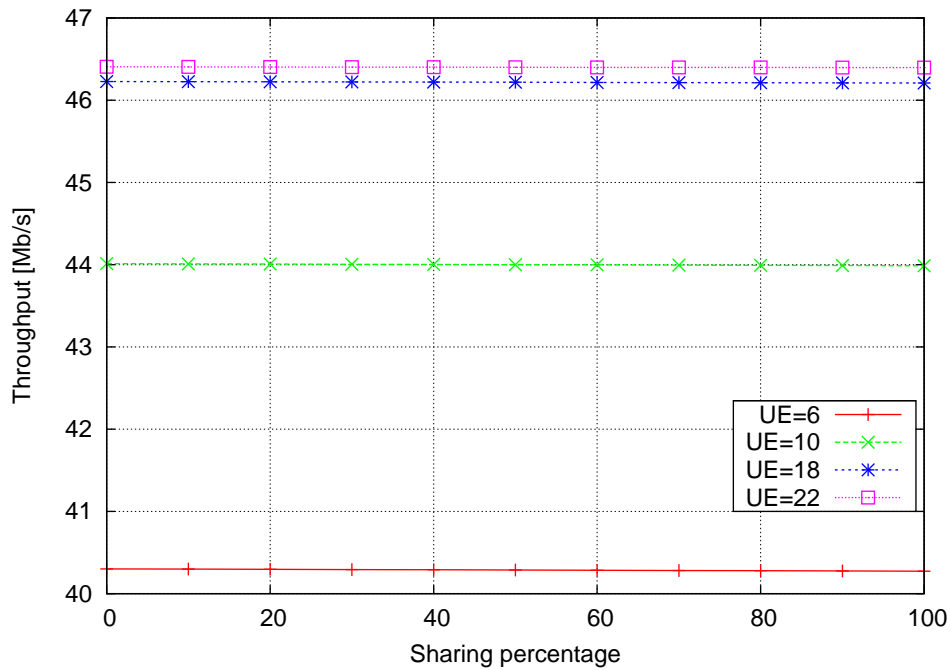


Figure 3.5: Cell throughput of the *max throughput* allocation

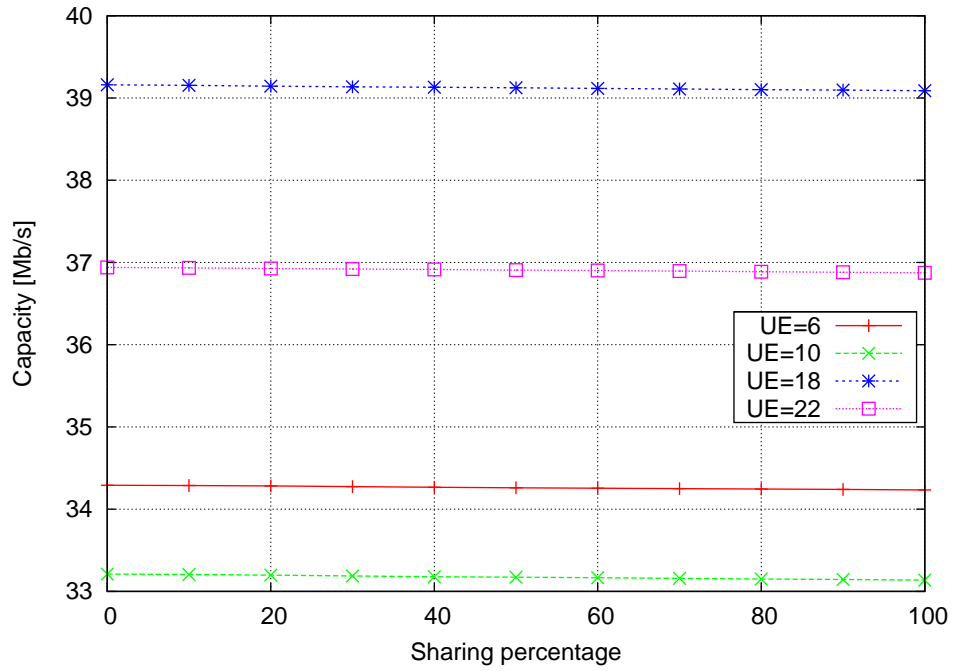


Figure 3.6: Cell capacity of the *fairness* allocation

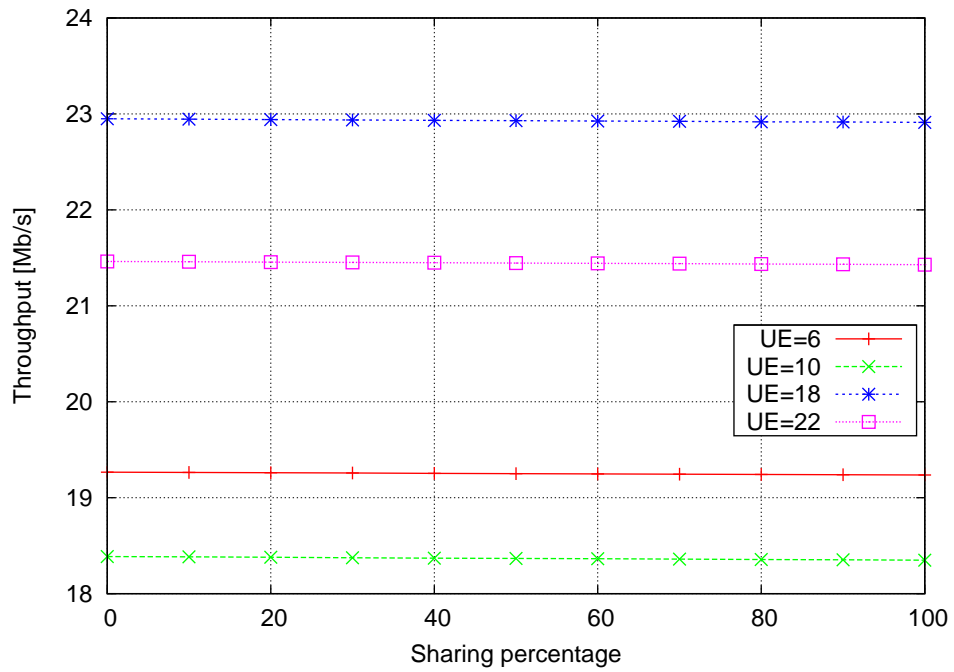


Figure 3.7: Cell throughput of the *fairness* allocation

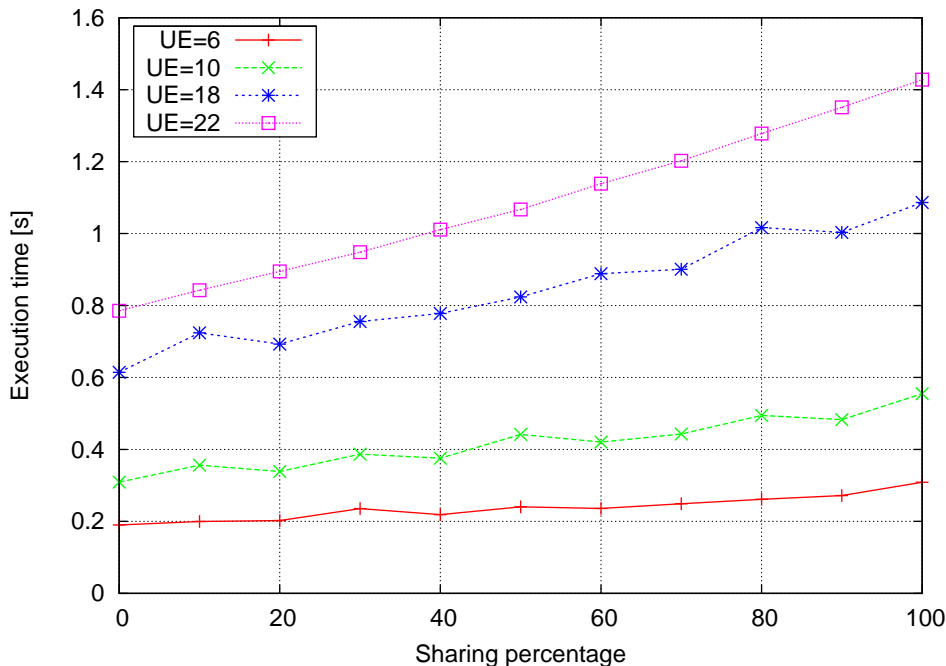


Figure 3.8: Simulation time

other approach, i.e. the *fairness* allocation, that aims at scheduling all the users, not just the best ones. As expected, applying a fair scheduling scheme results in a decrease of the system throughput, as is shown in Figures 3.6 and 3.7. Moreover, it is highlighted that in the *fairness* allocation both performance indices do not always improve when the number of users increases. In fact, when the number of users is increased, the fairness constraint is harder to satisfy and may actually lead to an overall decrease of the system capacity and throughput. This is an effect of the Round Robin intra-cell scheduling policy that we have proposed for the test. Of course, different policies lead to different results but the trade-off efficiency-versus-fairness cannot be avoided.

Finally, the execution time is analysed. As shown in Figure 3.8, there is an obvious complexity increase in the number of UEs and in the spectrum sharing percentage. A greater number of UEs requires more memory and computational resources to store and manage all the necessary objects and thus a higher execution time. On the other hand, a greater number of shared resources implies more contention and thus more iterations of the conflict resolution algorithm. Execution times also increase for higher sharing percentages, since the allocation algorithm has more degrees of freedom. Even though the values reported in the figure might seem too big, we want to remark that the tracing option was enabled during the simulation in order to log the performance indices and calculate statistics. Disk accesses are quite time consuming and can slow down the execution by more than 10 times the normal duration. However, in spite of all these points, the computational complexity scales almost linearly with the number of users and with the sharing percentage, and can thus be considered acceptable for realistic and detailed simulation campaigns.

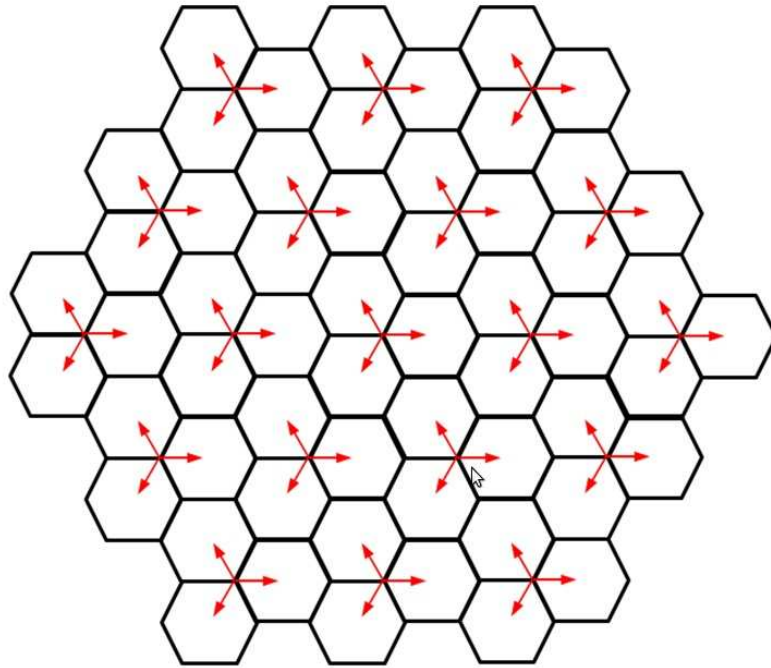


Figure 3.9: Scenario1 network layout

## 3.2 Simulation Framework for Evaluating Game-Theoretic Strategies

The evaluation of the game-theoretic strategies of partner WRC is based on the open source Network Simulator NS-2 [4] and its extension NS-MIRACLE [5], which was extended by the implementation of the Multi Carrier HSDPA radio interface, as well as corresponding MAC layer. In the following sub-sections, a detailed description of the tool is provided.

### 3.2.1 Network layout

The described tool is capable of generating one of two default (but not limited to these) homogeneous hexagonal grid scenarios, as listed below:

- Scenario1: Hexagonal grid, 3 sector/site, 19 sites/57 sectors, wrap around
- Scenario2: Hexagonal grid, 3 sector/site, 7 sites/21 sectors, wrap around

Each sector of the network is generated based on the antenna pattern as described in the following Subsection 3.2.1. Omni-directional sites can be generated as well, as omni-sites were the starting points for sectorized cells implementation.

In case of multi-operator scenarios, the initial step would be to model collocated operators with the same network layouts and independent spectrum resources configurations.

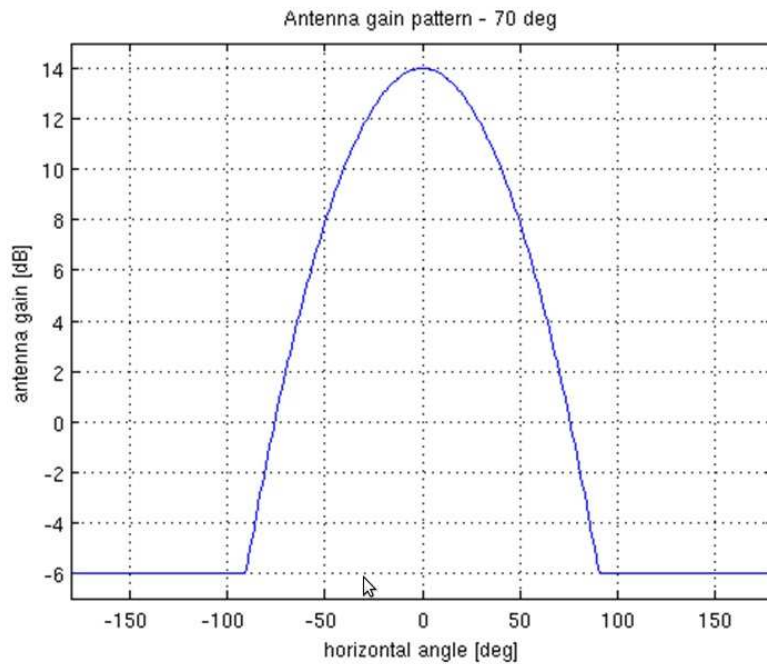


Figure 3.10: Antenna gain pattern

| Parameter                           | Value     |
|-------------------------------------|-----------|
| Shadowing distribution              | Lognormal |
| Shadowing standard deviation        | 8 dB      |
| Correlation distance of Shadowing   | 50 m      |
| Shadowing correlation Between cells | 0.5       |
| Between sites                       | 1.0       |

Table 3.3: Shadowing parameters

### Antenna pattern

The antenna pattern and gain was modeled according to the 3GPP model [6]. It assumes 2D pattern with 70 degree gain. The attenuation is limited to 20dB.

$$A(\theta) = -\min \left[ 12 \left( \frac{\theta}{\theta_{3dB}} \right)^2, A_m \right], \quad \theta_{3dB} = 70deg, \quad A_m = 30dB$$

In simulation parameters, a maximum antenna gain of 14 dBi was assumed. The final antenna gain pattern is depicted in Figure 3.9.

### Shadowing model

The system level simulator is designed to support mobility functionality. Therefore a shadowing map approach was used to determine shadow fading values. Shadowing parameters are assumed according to [6] (see Table 3.3).

| Channel type | No of taps | Taps coefficient                             | Taps delay        |
|--------------|------------|--|-------------------|
| Pedestrian A | 3          | -0.07, -19.27, -23.27                        | 0, 1, 2           |
| Vehicular A  | 6          | -3.14, -4.14, -12.14, -13.14, -18.14, -23.14 | 0, 1, 3, 4, 7, 10 |

Table 3.4: Fast Fading models

To assure the proper correlation values, shadowing maps were generated per site with grid of decorrelation distance and values from lognormal distribution. Additionally, one common map was generated and geometrically averaged with each site map (to assure 0.5 correlation between sites). Finally, shadowing values for each BS-MS link were linearly interpolated from appropriate site map.

### Multipath propagation models

In macro cell evaluation of MC-HSPA concepts, two fading models were considered:

- Pedestrian type A (PedA)
- Vehicular type A (VehA)

In multicarrier scenario, fading correlation equal to 0 was assumed.

### SINR model

WRC system level simulator models Type 2 (1Rx antenna, equalizer) and Type 3 (2Rx antenna, equalizer) receivers, using the following formulas:

$$SINR = SF_{16} \frac{P_k^{HS-DSCH}}{P_{intra} + \sum_{i \neq k} P_i^{inter} + P_{noise}}$$

$$P_{intra} = (P_k^{CPICH} + P_k^{common} + P_k^{HS-DSCH})(1 - \alpha) \quad (\alpha : \text{orthogonality factor}) \quad (3.4)$$

$$P_i^{inter} = P_i^{HS-DSCH} + P_i^{common} + P_i^{CPICH} \quad (3.5)$$

This approach treats the received signal power as sum of power on channel taps. In case of Type 3 receiver both channels are summed up. Own interferences are modeled using orthogonality factor (in range 0 - 1). Orthogonality factor values are dependent of user geometry, channel taps distribution (channel type) and current channel condition.

Therefore the orthogonality factor is represented by series of curves. Separate curve for each geometry (with granulation of 1dB) depicts orthogonality factor as a function of attenuation.

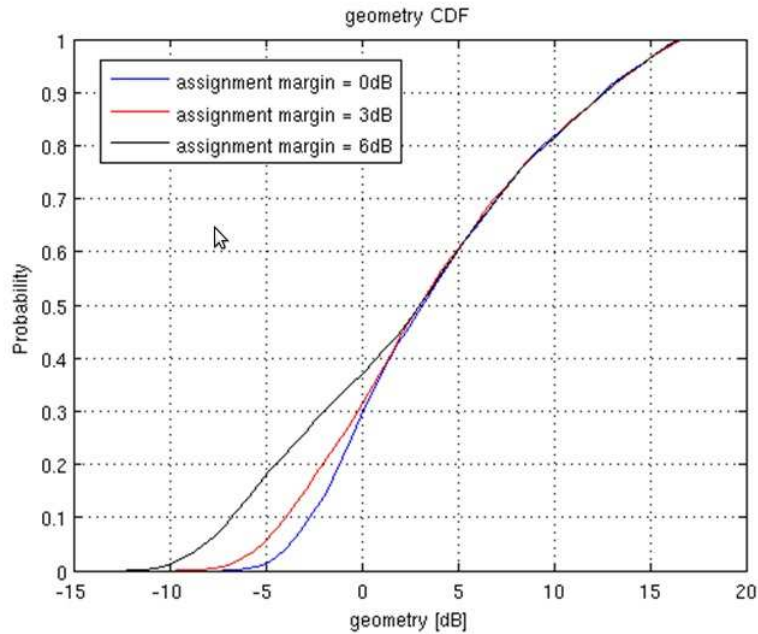


Figure 3.11: Geometry for different assignment margin settings

#### MS assignment procedure

User assignment to the cell is performed according to the following procedure:

1. User is randomly generated inside the network borders.
2. Loss is calculated to each cell (sum of pathloss, shadowing and antenna gain)
3. Minimum loss is found
4. Cells that fulfill condition:  $\text{loss} < (\text{minimum loss} + \text{assignment margin})$  are listed
5. Serving cell is selected randomly from the list
6. If max number of users for selected cell is not overcome then user is assigned and next user is generated (point 1), otherwise procedure is repeated for the same user.

Setting assignment margin to 0 dB provides to best cell selection. Other typical values are 3 or 6 dB. Results of different settings are depicted on Figure 3.11.

#### 3.2.2 Scheduler design

In this chapter, we describe proportional fair scheduler design, used in the simulations. The main principle of proportional fair scheduling is that, at each Transmission Time Interval (TTI), the user to be scheduled will be the one showing

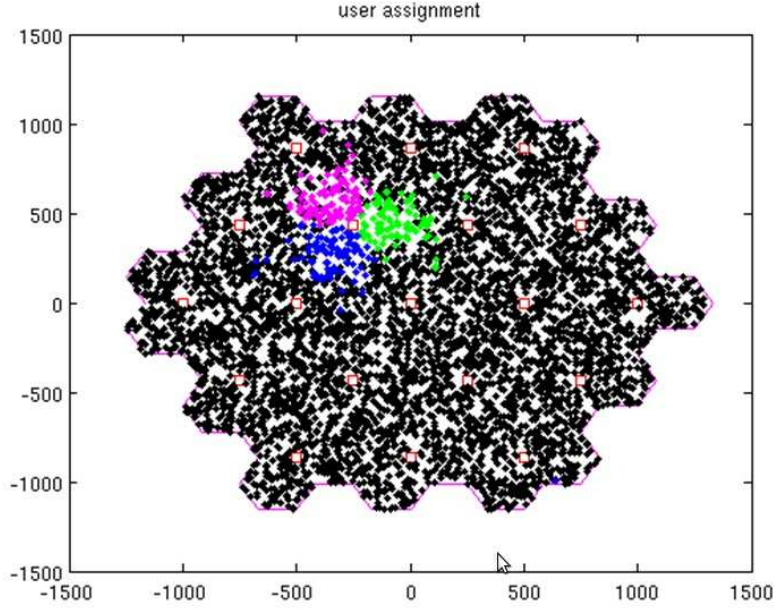


Figure 3.12: Example user assignment realization

maximum priority, computed as follows:

$$\frac{R_{request}}{R_{served}}, \quad (3.6)$$

where  $R_{request}$  is the instantaneous requested rate based on SINR and  $R_{served}$  is the average served data rate up to the previous TTI, computed as the Infinite Impulse Response (IIR) filtered average of instantaneous served rate  $R'_{served}$  Reserved with time constant  $T_c$ :

$$R_{served} = \frac{R'_{served}}{T_c} + \left(1 - \frac{1}{T_c}\right) R_{served} \quad (3.7)$$

For the Dual Carrier case, the priorities are calculated individually per carrier. The  $R_{served}$  value can be independent on each carrier or represent the total served throughput among all carriers, depending on a input parameter.

### Input Parameters

Modifications in the algorithm can be done using the following parameters:

- Bool commonDenominator: when set to 1, algorithm is executed with common  $R_{served}$  for all carriers (served throughput among all carriers accounted), otherwise, served throughput is considered independently per carrier.
- Double dFilterWindow: number of TTI representing  $T_c$  (currently set for 340 0.68s);
- Bool priorityToRetransmissions: when set to 1, users with packets to be retransmitted are given priority over the others. Execution The scheduling

algorithm is executed  $N$  times, assuming  $N$  equals the number of carriers. After one user is chosen to be scheduled on each carrier the average served throughput,  $R_{served}$ , is updated according to (3.7). For each carrier, the algorithm is repeated until a valid user is found or there is no user fulfilling the requirements for being scheduled. A user is considered valid if:

- It is capable of receiving data ( $R_{requested} > 0$ ) AND
- It has not been scheduled more than `uMaxNumberOfCarriersPerUser` times AND
- It has pending retransmissions OR
- It has pending data in the queue that has not been already scheduled in previous carriers in this TTI An algorithm flow is shown below:

#### Parameterisation

Overall simulation parameters and assumptions are based on [6] and [7].

### 3.3 Asymptotic Analysis Assessment

In this section we report the results obtained by the implementation of a sharing algorithm that enables the assessment of the asymptotic sharing gain of the operators in the case of orthogonal spectrum sharing. The scenario is exactly the same considered in the Section 3.1. The simulator used is the ns-3 with all the customisations described in that section, and also the performance metrics used are the same.

We have evaluated the upper bound on the sharing gain that can be achieved by resorting to a centralised approach. Despite its inapplicability in a real scenario, it is useful from a theoretical point of view. In particular, we have implemented a *Monopoly-like upper bound algorithm* that maximises the total joint capacity. In other words, the operators behave as if they were a single entity (a monopolist). No balancing is taken into consideration. Each AT is always assigned to the best UE: for the common pool it does not matter the eNB it belongs to, while for the private parts of the spectrum only UEs registered to that frequencies' owner can be chosen. In this way, the actual capacity obtained is the maximum one, a theoretical upper bound.

Figure 3.14 shows the sum capacity that can be achieved for a different number of UEs per cell when the spectrum sharing increases. Several consideration can be done by looking at that figure. Of course, in this case there is a clear increase in the capacity with the number of users due to the multiuser diversity, as discussed for the sharing policies already presented in Section 3.1.4. Besides that, the most important consideration that can be done is that there is a neat *sharing gain*. The sum capacity increases with the sharing percentage, thus the network operators have an incentive in sharing part of their frequencies. For a small number of UEs

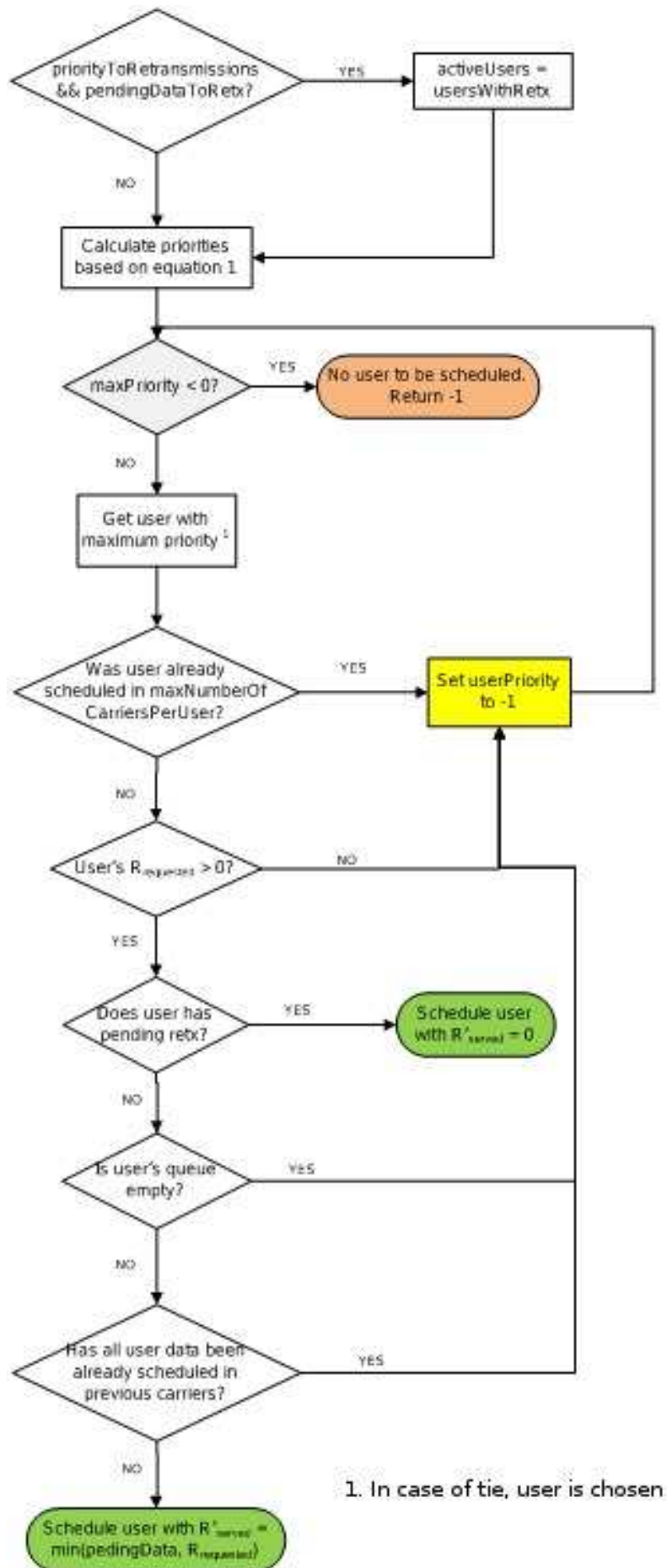


Figure 3.13: Proportional fair scheduler flow

| Parameter                        | Value and comment   |
|----------------------------------|---|
| Network layout                   | Hexagonal grid, 3 sector/site, 19 sites/57 sectors, wrap around |
| Inter site distance (ISD)        | 500 m   |
| Neighbour cell modeling          | Users modelled in whole network                                 |
| Cell Isolation                   | 0 dB  |
| Wrap around                      | Yes   |
| Carrier frequency                | 2 GHz   |
| Number of bands                  | 1; Inband case  |
| Antenna configuration            | 3 sector  |
| Antenna beamwidth                | 70 deg  |
| Antenna Front To Back ratio      | 20 dB   |
| Node B antenna gain              | 14 dBi  |
| Node B TX power                  | 43 dBm  |
| Minimum MS-BS distance           | 35m   |
| Propagation model                | $128.1 + 37.6\log_{10}(R)$                                      |
| Shadowing                        | 8 dB standard deviation   |
| Shadowing correlation            | 1 between sectors, 0.5 between sites                            |
| Penetration loss                 | 0 dB  |
| Thermal noise level              | -102.9dBm   |
| Channel models                   | PedA 3km/h, VehA 3km/h Fading across carriers is uncorrelated   |
| Number of users per sector       | Variable (default: 10 UEs) Uniform distribution, randomized     |
| MS noise figure                  | 9 dB  |
| MS RX Type                       | Type2, Type3  |
| MS capabilities                  | 15 SF 16 codes capable per carrier                              |
| MS antenna gain                  | 0 dB, omni  |
| User positioning                 | Random, reset 10 times during the simulation (#drops)           |
| Simulation time                  | At least 10 seconds per drop                                    |
| MCS set                          | 30 MCS; 1 - 2dB granularity                                     |
| QoS                              | 10% BLER after first transmission                               |
| Transmission Time Interval (TTI) | 2 ms  |
| Scheduler configuration          | Round Robin, Proportional Fair, Joint queue                     |
| Number of HARQ processes         | 6 asynchronous  |
| Number of HARQ retransmissions   | up to 4 not prioritized retransmissions                         |
| CQI estimation error             | normal distribution, 1 dB std                                   |
| CQI reporting delay              | 3 TTI   |
| BS height                        | 30m   |
| MS height                        | 1,5m  |

Table 3.5: Simulation parameters

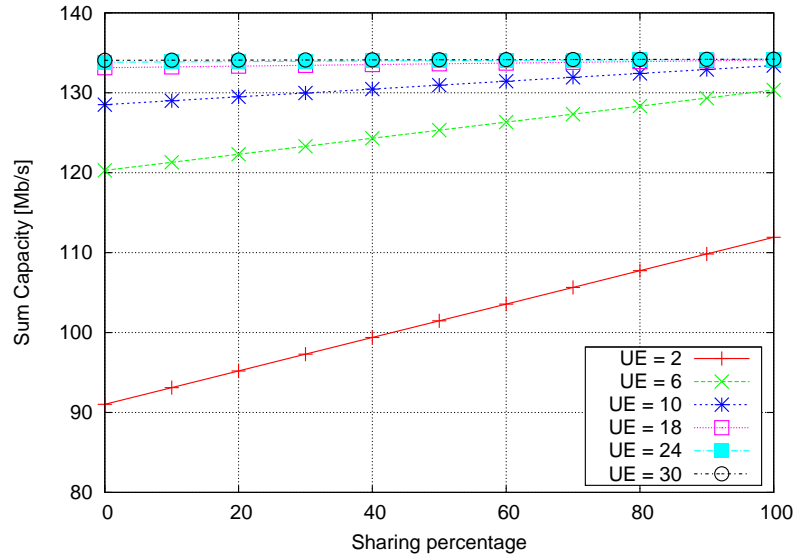


Figure 3.14: Theoretical upper bound on the sum capacity

the increment of capacity can reach up to 20% of the no-sharing solution. The fact that the marginal gain decreases with the number of UEs is still a consequence of the reduced multiuser diversity: after a certain point both the operators always have at least an UE with a good CQI for each subchannel thus there is no interest for them in accessing each other's resources.

However, it is important to remind that these values have been obtained for a scenario under saturation, which is typically the worst condition that one can consider. In the case of low-loaded networks, an eNB may have only few active flows at each allocation slot and thus the other eNB could opportunistically exploit most of the resources that are not used. According to this consideration, we can consider the results presented in Figure 3.14 as the worst-case upper bound.



## 4 Conclusions and Discussion of Next Steps

The main outcomes of this report are summarised in the Executive Summary (Chapter 1). The presented methods cover different aspects and functionalities of a wireless communication system, ranging from physical layer modelling up to networking aspects. These activities involve different partners of WP4, and they depend on the outputs of other WPs. In particular, the simulation methodologies will be used in the 3rd year for testing the algorithms that were developed in WP2, WP3, and WP4. This cooperation also involves WP6 (hardware platform) where propagation channels were measured and simulated.

The focus of the 3rd year of SAPHYRE will be on a joint system level simulation, based on the results obtained thus far. This requires a joint effort spanning all WPs of SAPHYRE. This overall approach for SAPHYRE system level simulations is illustrated in Figure 4.1.

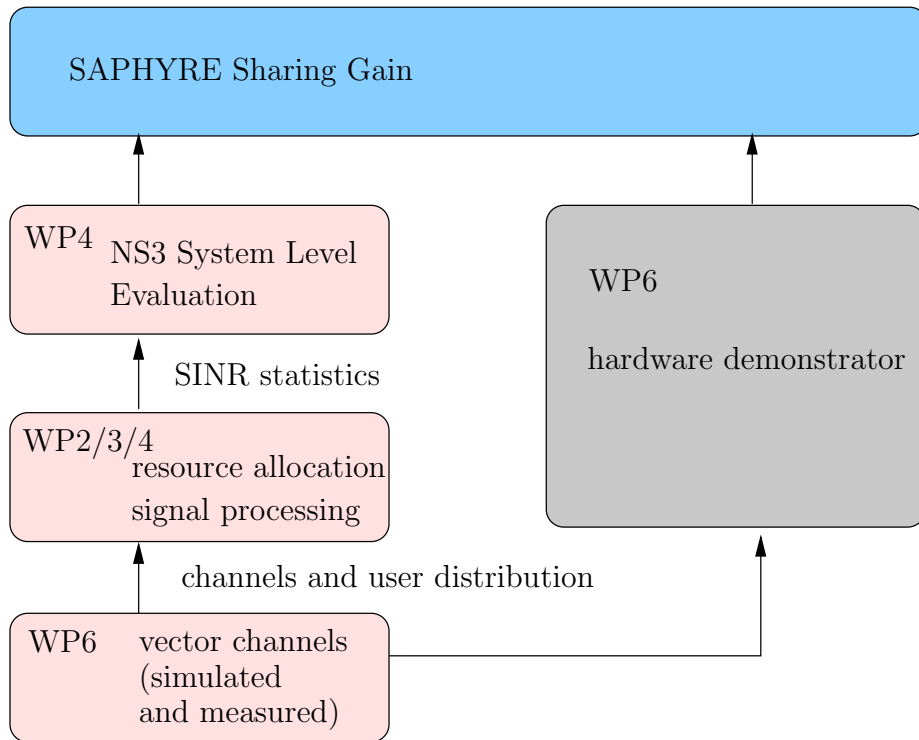


Figure 4.1: Outlook for the 3rd year of SAPHYRE: cross-workpackage approach to system level evaluation

The propagation channels are provided by WP6. They are either simulated by the SCME channel model developed in the IST WINNER project [16] or measured by using the WP6 hardware testbed. In both cases, reference channels are stored. Based on these channels and reference topologies (user distributions), SINR statis-

#### *4 Conclusions and Discussion of Next Steps*

tics are computed with the algorithms from WP2, WP3, and WP4. This SINR statistic provides the basis for the system level simulation carried out with NS3.

This approach enables a cross-layer evaluation of the SAPHYRE sharing. It includes realistic propagation channels, and the relevant PHY/MAC technologies like scheduling and beamforming, which are crucial for resource sharing.

## Bibliography

- [1] Evolved Universal Terrestrial Radio Access (E-UTRA); Radio Frequency (RF) system scenarios', v8.1.0, 2008.
- [2] 3GPP Evolved Universal Terrestrial Radio Access (E-UTRA); Overall description; Stage 2, 3GPP TS 36.300.
- [3] 3GPP Tech. Specif. Group Radio Access Network; Conveying MCS and TB size via PDCCH, 3GPP TSG-RAN WG1 R1-081483.
- [4] [http://nsgam.isi.edu/nsgam/index.php/Main\\_Page](http://nsgam.isi.edu/nsgam/index.php/Main_Page) - NS-2 website.
- [5] <http://www.dei.unipd.it/wdyn/?IDsezione=3966> - NS-MIRACLE website.
- [6] TR-25.814, Physical layer aspects for evolved Universal Terrestrial Radio Access (UTRA) (Release 7), V7.1.0, September 2006.
- [7] R1-081706, Simulation Assumptions for DC HSDPA Performance Evaluations, Qualcomm Europe, Ericsson, Nokia, Nokia Siemens Networks, 3GPP TSG-RAN WG1 no. 53, May 2008.
- [8] ns-3 simulator, available at: <http://www.nsgam.org/>.
- [9] FP7 SAPHYRE Sharing Physical Resources - Mechanisms and Implementations for Wireless Networks. project (FP7-ICT-248001), 2011.
- [10] 3GPP TR 25.996 V10.0.0. Spatial channel model for multiple input multiple output (MIMO) simulations (release 10), mar 2011.
- [11] 3GPP TS 36.211 V9.1.0. E-UTRA - physical channels and modulation (release 9), March 2010.
- [12] Luca Anchora, Leonardo Badia, and Michele Zorzi. Joint Scheduling and Resource Allocation for LTE Downlink Using Nash Bargaining Theory. In *Proc. of IEEE International Conference on Communications (ICC)*, 2011.
- [13] Luca Anchora, Marco Mezzavilla, Leonardo Badia, and Michele Zorzi. Simulation Models for the Performance Evaluation of Spectrum Sharing Techniques in OFDMA Networks. In *Proc. of the 14th ACM International Conference on Modeling, Analysis and Simulation of Wireless and Mobile Systems (MSWiM)*, 2011.
- [14] Thomas Bonald. A score-based opportunistic scheduler for fading radio channels. *5th European Wireless Conference*, February 2004.

- [15] H. Claussen. Efficient modelling of channel maps with correlated shadow fading in mobile radio systems. In *Personal, Indoor and Mobile Radio Communications, 2005. PIMRC 2005. IEEE 16th International Symposium on*, volume 1, pages 512–516, sept. 2005.
- [16] L. Hentilä, P. Kyösti, M. Kiskala, M. Narandzic, and M. Alatossava. MATLAB implementation of the WINNER Phase II Channel Model ver1.1. Technical report, December 2007.
- [17] IST-4-027756, WINNER II. D6.11.2, Key scenarios and implications for WINNER II. Technical report, 2006.
- [18] IST-4-027756, WINNER II. D1.1.2, WINNER II channel models. Technical report, 2007.
- [19] IST-4-027756, WINNER II. D2.2.3, Modulation and Coding schemes for the WINNER II System. Technical report, 2007.
- [20] Allen MacKenzie and Luiz DaSilva. *Game Theory for Wireless Engineers*. Morgan and Claypool, San Rafael, CA, 2006.
- [21] Giuseppe Piro, Nicola Baldo, and Marco Miozzo. An LTE Module for the ns-3 Network Simulator. In *Workshop on NS-3*, 2011.
- [22] W. Rhee and J.M. Cioffi. Increase in capacity of multiuser ofdm system using dynamic subchannel allocation. In *IEEE 51st Vehicular Technology Conference Proceedings, 2000. VTC 2000-Spring Tokyo.*, volume 2, pages 1085–1089 vol.2, 2000.
- [23] Malte Schellmann, Lars Thiele, Volker Jungnickel, and Thomas Haustein. A fair score-based scheduler for spatial transmission mode selection. *IEEE 41st Asilomar Conference on Signals, Systems and Computers*, November 2007.
- [24] Lars Thiele, Thomas Wirth, Kai Börner, Michael Olbrich, Volker Jungnickel, Juergen Rumold, and Stefan Fritze. Modeling of 3D Field Patterns of Down-tilted Antennas and Their Impact on Cellular Systems. *International ITG Workshop on Smart Antennas (WSA 2009)*, February 2009.
- [25] P. Viswanath, D.N.C. Tse, and R. Laroia. Opportunistic beamforming using dumb antennas. *Information Theory, IEEE Transactions on*, 48(6):1277–1294, 2002.